

CERN-EP-2017-168
2018/02/06

CMS-HIG-17-006

Search for resonant and nonresonant Higgs boson pair production in the $b\bar{b}\ell\nu\ell\nu$ final state in proton-proton collisions at $\sqrt{s} = 13$ TeV

The CMS Collaboration*

Abstract

Searches for resonant and nonresonant pair-produced Higgs bosons (HH) decaying respectively into $\ell\nu\ell\nu$, through either W or Z bosons, and $b\bar{b}$ are presented. The analyses are based on a sample of proton-proton collisions at $\sqrt{s} = 13$ TeV, collected by the CMS experiment at the LHC, corresponding to an integrated luminosity of 35.9 fb^{-1} . Data and predictions from the standard model are in agreement within uncertainties. For the standard model HH hypothesis, the data exclude at 95% confidence level a product of the production cross section and branching fraction larger than 72 fb , corresponding to 79 times the standard model prediction. Constraints are placed on different scenarios considering anomalous couplings, which could affect the rate and kinematics of HH production. Upper limits at 95% confidence level are set on the production cross section of narrow-width spin-0 and spin-2 particles decaying to Higgs boson pairs, the latter produced with minimal gravity-like coupling.

Published in the Journal of High Energy Physics as doi:10.1007/JHEP01(2018)054.

1 Introduction

The Brout–Englert–Higgs mechanism is a key element of the standard model (SM) of elementary particles and their interactions, explaining the origin of mass through spontaneous breaking of electroweak symmetry [1–6]. The discovery of a Higgs boson with a mass m_H around 125 GeV by the ATLAS and CMS experiments [7–9] fixes the value, in the SM, of the self-coupling λ in the scalar potential, whose shape is determined by the symmetries of the SM and the requirement of renormalisability. Direct information on the Higgs three- and four-point interactions will provide an indication of the scalar potential structure.

Nonresonant Higgs boson pair production (HH) can be used to directly study the Higgs boson self-coupling. At the CERN LHC, Higgs boson pairs are predominantly produced through gluon-gluon fusion via two destructively interfering diagrams, shown in Fig. 1. In the SM the destructive interference between these two diagrams makes the observation of HH production extremely challenging, even in the most optimistic scenarios of energy and integrated luminosity at the future High Luminosity LHC [10, 11]. The SM cross section for HH production in proton-proton collisions at $\sqrt{s} = 13$ TeV for a Higgs boson mass of 125 GeV is $\sigma^{\text{HH}} = 33.5$ fb at next-to-next-to-leading order (NNLO) in quantum chromodynamics (QCD) for the gluon-gluon fusion process [12–21].

Indirect effects at the electroweak scale arising from beyond the standard model (BSM) phenomena at a higher scale can be parameterised in an effective field theory framework [22–24] by introducing coupling modifiers for the SM parameters involved in HH production, namely $\kappa_\lambda = \lambda/\lambda_{\text{SM}}$ for the Higgs boson self-coupling λ and $\kappa_t = y_t/y_{t_{\text{SM}}}$ for the top quark Yukawa coupling y_t . Such modifications of the Higgs boson couplings could enhance Higgs boson pair production to rates observable with the current dataset. The relevant part of the modified Lagrangian takes the form:

$$\mathcal{L}_H = \frac{1}{2} \partial_\mu H \partial^\mu H - \frac{1}{2} m_H^2 H^2 - \kappa_\lambda \lambda_{\text{SM}} v H^3 - \frac{m_t}{v} (v + \kappa_t H) (\bar{t}_L t_R + \text{h.c.}), \quad (1)$$

where H is the Higgs boson field, v is the vacuum expectation value of H , m_t is the top quark mass, \bar{t}_L and t_R are the left- and right-handed top quark fields, and h.c. is the Hermitian conjugate. The appearance of new contact-like interactions, not considered in this paper, could also result in an enhancement of HH production.

Extensions of the scalar sector of the SM postulate the existence of additional Higgs bosons. An explored scenario is the two-Higgs-doublet model (2HDM) [25], where a second doublet of complex scalar fields is added to the SM scalar sector Lagrangian. The generic 2HDM potential has a large number of degrees of freedom, which can be reduced to six under specific assumptions. In case the new CP-even state is massive enough (mass larger than $2m_H$) it can decay to a pair of Higgs bosons. Models inspired by warped extra dimensions [26] predict the existence of new heavy particles that can decay to pairs of Higgs bosons. Examples of such particles are the radion (spin 0) [27–30] or the first Kaluza–Klein (KK) excitation of the graviton (spin 2) [31, 32]. In the following, we will use X to denote a generic state decaying into pairs of Higgs bosons.

Searches for Higgs boson pair production have been performed by the ATLAS and CMS experiments using LHC proton-proton collision data. These include searches for BSM production as well as more targeted searches for production with SM-like kinematics in $\sqrt{s} = 8$ TeV [33–37] and 13 TeV data [38, 39].

This paper reports on a search for Higgs boson pair production, HH, and resonant Higgs boson pair production, $X \rightarrow HH$, where one of the H decays into $b\bar{b}$, and the other into $Z(\ell\bar{\ell})Z(\nu\nu)$

or $W(\ell\nu)W(\ell\nu)$, where ℓ is either an electron, a muon, or a tau lepton that decays leptonically. The search is based on LHC proton-proton collision data at $\sqrt{s} = 13$ TeV collected by the CMS experiment, corresponding to an integrated luminosity of 35.9 fb^{-1} . The analysis focuses on the invariant mass distribution of the b jet pairs, searching for a resonant-like excess compatible with the Higgs boson mass, in combination with an artificial neural network discriminator based on kinematic information. The dominant background is $t\bar{t}$ production, with smaller contributions from Drell–Yan (DY) and single top quark production.

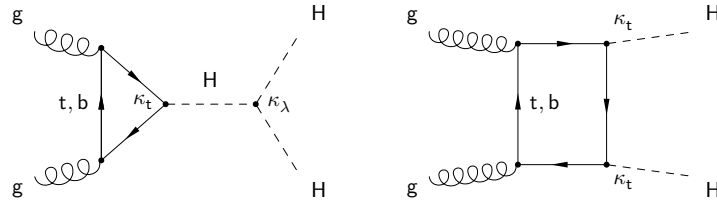


Figure 1: Feynman diagrams for Higgs boson pair production via gluon fusion in the SM. The coupling modifiers for the Higgs boson self-coupling and the top quark Yukawa coupling are denoted by κ_λ and κ_t , respectively.

2 The CMS detector

The central feature of the CMS apparatus is a superconducting solenoid of 6 m internal diameter, providing a magnetic field of 3.8 T. Within the solenoid volume are a silicon pixel and strip tracker, a lead tungstate crystal electromagnetic calorimeter (ECAL), and a brass and scintillator hadron calorimeter, each composed of a barrel and two endcap sections. Forward calorimeters extend the pseudorapidity coverage provided by the barrel and endcap detectors. Muons are detected in gas-ionisation chambers embedded in the steel flux-return yoke outside the solenoid. A more detailed description of the CMS detector, together with a definition of the coordinate system used and the relevant kinematic variables, can be found in Ref. [40].

3 Event simulation

The main background processes, in decreasing order of importance, are $t\bar{t}$, DY, and single top quark production. Diboson, triboson, $t\bar{t}V$ and SM single Higgs boson production are also considered. Other contributions, such as W +jets or QCD multijet events with jets misidentified as leptons, are negligible due to the dilepton selection described in the next section. The dominant contribution, especially in the $e^\pm\mu^\mp$ channel, arises from $t\bar{t}$ production yielding the same final state as the signal process (two b quark jets, two leptons, and two neutrinos) when both W bosons from top quark decays further decay leptonically.

Background simulation samples have been generated at next-to-leading order (NLO) in QCD using POWHEG 2 [41–45], and MADGRAPH5_aMC@NLO versions 2.2.2.0 and 2.3.2.2 [46] with FxFx merging [47] and MADSPIN [48]. The signal samples of gluon fusion production of two Higgs bosons, and of spin-0 or spin-2 narrow resonances decaying into two Higgs bosons, have been generated at leading order (LO) in QCD using MADGRAPH5_aMC@NLO version 2.2.2.0. The spin-2 narrow resonance is produced as a KK-graviton with minimal coupling [49], leading to spin projection ± 2 on the beam axis. The mass of the Higgs boson has been fixed to

125 GeV [50], and its branching fractions to those in the SM. One of the Higgs bosons is required to decay into a pair of b quarks, while the second one is required to decay to final states containing two leptons and two neutrinos of any flavour. This implies that the signal samples contain both $H \rightarrow Z(\ell\ell)Z(\nu\nu)$ and $H \rightarrow W(\ell\nu)W(\ell\nu)$ decay chains, leading to a total branching fraction $\mathcal{B}(HH \rightarrow b\bar{b}VV \rightarrow b\bar{b}\ell\nu\ell\nu)$ of 2.7% [12]. The event generators used for both signal and background samples are interfaced with PYTHIA 8.212 [51, 52] for simulation of the parton showering, hadronisation, and underlying event using the CUETP8M1 tune [53]. The NNPDF 3.0 [54] LO and NLO Parton Distribution Functions (PDF) are used.

For all processes, the detector response is simulated using a detailed description of the CMS apparatus, based on the GEANT4 package [55]. Additional pp interactions in the same and in the neighbouring bunch crossings (pileup) are generated with PYTHIA and overlapped with the simulated events of interest to reproduce the pileup measured in data.

All background processes are normalised to their most accurate theoretical cross sections. The $t\bar{t}$, DY, single top quark and W^+W^- samples are normalised to NNLO precision in QCD [56–59], while remaining diboson, triboson and $t\bar{t}V$ processes are normalised to NLO precision in QCD [46, 60]. The single Higgs boson production cross section is computed at the NNLO precision of QCD corrections and NLO precision of electroweak corrections [12].

4 Event selection and background predictions

Data are collected with a set of dilepton triggers. The p_T thresholds applied by the triggers are asymmetric and channel-dependent, and vary from 17 to 23 GeV for the leading leptons and from 8 to 12 GeV for the subleading leptons. Trigger efficiencies are measured with a “tag-and-probe” technique [61] as a function of lepton p_T and η in a data control region consisting of $Z \rightarrow \ell\ell$ events.

Events with two oppositely charged leptons (e^+e^- , $\mu^+\mu^-$, $e^\pm\mu^\mp$) are selected using asymmetric p_T requirements, chosen to be above the corresponding trigger thresholds, for leading and subleading leptons of 25 GeV and 15 GeV for ee and μe events, 20 GeV and 10 GeV for $\mu\mu$ events, and 25 GeV and 10 GeV for $e\mu$ events. Electrons in the pseudorapidity range $|\eta| < 2.5$ and muons in the range $|\eta| < 2.4$ are considered.

Electrons, reconstructed by associating tracks with ECAL clusters, are identified by a sequential selection using information on the cluster shape in the ECAL, track quality, and the matching between the track and the ECAL cluster. Additionally, electrons from photon conversions are rejected [62]. Muons are reconstructed from tracks found in the muon system, associated with tracks in the silicon tracking detectors. They are identified based on the quality of the track fit and the number of associated hits in the different tracking detectors [63]. The lepton isolation, defined as the scalar p_T sum of all particle candidates in a cone around the lepton, excluding the lepton itself, divided by the lepton p_T , is required to be < 0.04 for electrons (with a cone of radius $\Delta R = \sqrt{(\Delta\phi)^2 + (\Delta\eta)^2} = 0.3$) and < 0.15 for muons (with a cone of radius $\Delta R = 0.4$). Lepton identification and isolation efficiencies in the simulation are corrected for residual differences with respect to data. These corrections are measured in a data sample, enriched in $Z \rightarrow \ell\ell$ events, using a “tag-and-probe” method and are parameterised as a function of lepton p_T and η .

Jets are reconstructed using a particle flow (PF) technique [64]. PF candidates are clustered to form jets using the anti- k_T clustering algorithm [65] with a distance parameter of 0.4, implemented in the FASTJET package [66]. Jet energies are corrected for residual nonuniformity and

nonlinearity of the detector response [67]. Jets are required to have $p_T > 20 \text{ GeV}$, $|\eta| < 2.4$, and be separated from identified leptons by a distance of $\Delta R > 0.3$. The missing transverse momentum vector, defined as the projection onto the transverse plane relative to the beam axis, of the negative vector sum of the momenta of all PF candidates, is referred to as \vec{p}_T^{miss} [68, 69]. Its magnitude is denoted by p_T^{miss} . Corrections to the jet energies are propagated to \vec{p}_T^{miss} .

The reconstructed vertex with the largest value of summed object p_T^2 is taken to be the primary pp interaction vertex, considering the objects returned by a clustering algorithm applied to all charged tracks associated with the vertex, plus the corresponding associated \vec{p}_T^{miss} .

The combined multivariate algorithm [70, 71] is used to identify jets originating from b quarks. Jets are considered as b tagged if they pass the medium working point of the algorithm, which provides around 70% efficiency with a mistag rate less than 1%. Correction factors are applied in the simulation to the selected jets to account for the different response of the combined multivariate algorithm between data and simulation [71]. Among all possible dijet combinations fulfilling the previous criteria, we select the two jets with the highest combined multivariate algorithm outputs.

After the final object selection consisting of two opposite sign leptons and two b-tagged jets, a requirement of $12 < m_{\ell\ell} < m_Z - 15 \text{ GeV}$ is applied to suppress quarkonia resonances and jets misidentified as leptons, and to remove the large background at the Z boson peak as well as the high- $m_{\ell\ell}$ tail of the DY and $t\bar{t}$ processes. This requirement has a negligible impact on signal events where one H decays as $H \rightarrow W(\ell\nu)W(\ell\nu)$, and removes only the portion of $H \rightarrow Z(\ell\ell)Z(\nu\nu)$ decays with on-shell Z($\ell\ell$) legs. Figure 2 shows the dijet p_T for data and simulated events after requiring the selection criteria described in this section.

All the background processes are estimated from simulation, with the exception of DY production in the e^+e^- and $\mu^+\mu^-$ channels. The DY contribution in the $e^\pm\mu^\mp$ channels is almost negligible, and is taken from simulation.

The contribution of the DY process in the analysis selection is estimated from a data sample enriched in DY plus jets events. The estimate is performed by requiring all the selection criteria described above, except for the b tagging requirements. The resulting dataset is corrected with weights to represent the DY contribution in the full selection. The weights are a function of kinematic variables and are tuned to reproduce the effect of applying the b tagging requirements on the DY process. They account for the following features:

- The b tagging efficiencies are not constant and depend on jet kinematics. Moreover, this dependency is different for b-, c- or light-flavour jets.
- The relative contributions of DY plus two jets of flavours k and l , where $k, l = \text{b, c, or light-flavour}$, to the DY plus two jets process are not constant throughout the phase-space. Modelling the effect of b tagging requires to parameterise the fractions F_{kl} of jets with flavours k and l as a function of event kinematics.

We compute the weights as:

$$W_{\text{sim}} = \sum_{k,l=\text{b,c,light-flavour}} F_{kl}(\text{BDT}) \epsilon_k(p_T^{j_1}, \eta^{j_1}) \epsilon_l(p_T^{j_2}, \eta^{j_2}), \quad (2)$$

where ϵ_k and ϵ_l are the b tagging efficiencies for k - and l -flavour jets calculated from simulation as a function of p_T and η of the jets and corrected for differences between data and simulation, and j_1 and j_2 denote the two p_T -ordered jets selected according to the above requirements. The expected fractions of jets with flavours k and l in the dataset are denoted by F_{kl} and are parameterised as a function of the output value of a Boosted Decision Tree (BDT) [72]. The indices k

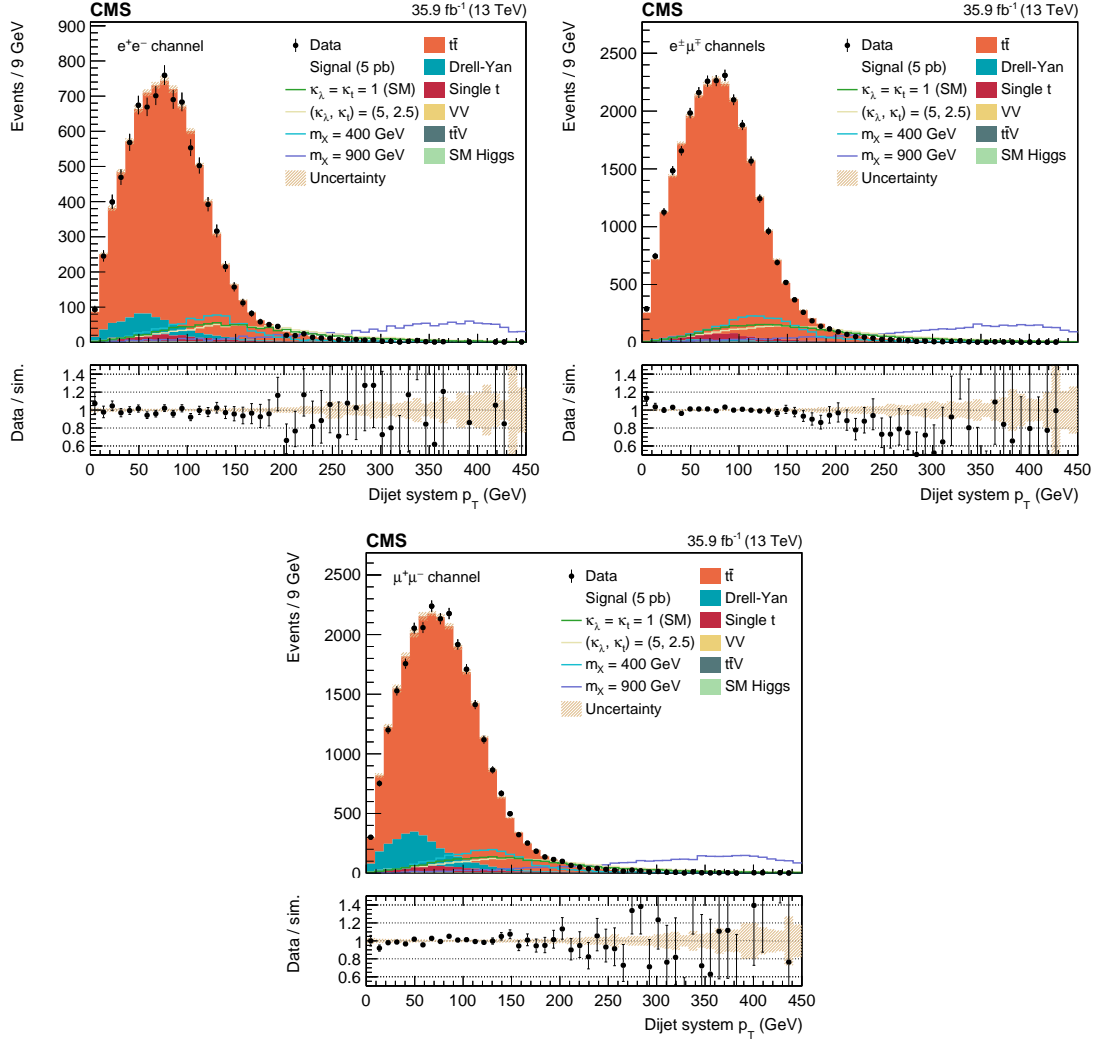


Figure 2: The dijet p_T distributions in data and simulated events after requiring two leptons, two b -tagged jets, and $12 < m_{\ell\ell} < m_Z - 15$ GeV, for e^+e^- (top left), $e^\pm\mu^\mp$ (top right), and $\mu^+\mu^-$ (bottom) events. The various signal hypotheses displayed have been scaled to a cross section of 5 pb for display purposes. Error bars indicate statistical uncertainties, while shaded bands show post-fit systematic uncertainties.

and l refer to the assumed flavour of j_1 and j_2 , respectively. The flavour fractions F_{kl} are estimated from a simulated DY sample. Their dependency on the BDT output value accounts for the different kinematical behaviours of heavy- or light-flavour associated DY processes, effectively reducing the dimensionality of the phase-space to a single variable. The BDT is trained to discriminate $DY+b\bar{b}, c\bar{c}$ from other DY associated production processes using the following input variables: $p_T^{j_1}, p_T^{j_2}, \eta^{j_1}, \eta^{j_2}, p_T^{\ell\ell}, p_T^{\ell\ell}, \eta^{\ell\ell}, \Delta\phi(\ell\ell, \vec{p}_T^{\text{miss}})$ (defined as the $\Delta\phi$ between the dilepton system and \vec{p}_T^{miss}), number of jets, and H_T defined as the scalar sum of the transverse momentum of all selected leptons and jets.

Beside DY, the data sample without b tagging requirements contains small contributions from other backgrounds such as $t\bar{t}$, single top quark and diboson production. Hence, the same reweighting procedure is applied to simulated samples for these processes, and the result is subtracted from the weighted data to define the estimate of the DY background in the analysis region.

The method is validated both in simulation and in two data control regions requiring either $m_{\ell\ell} > m_Z - 15 \text{ GeV}$ or $|m_{\ell\ell} - m_Z| < 15 \text{ GeV}$. The predicted DY distributions are in agreement with data and simulation within the uncertainties of the method, described in section 6.

5 Parameterised multivariate discriminators for signal extraction

Deep neural network (DNN) discriminators, based on the Keras library [73], are used to improve the signal-to-background separation. As the dominant background process ($t\bar{t}$ production) is irreducible, the DNNs rely on information related to event kinematics. The variables provided as input to the DNNs exploit the presence in the signal of two Higgs bosons decaying into two b jets on the one hand, and two leptons and two neutrinos on the other hand, which results in different kinematics for the dilepton and dijet systems between signal and background processes. The variables used as input are: $m_{\ell\ell}$, $\Delta R_{\ell\ell}$, ΔR_{jj} , $\Delta\phi(\ell\ell, jj)$ (defined as the $\Delta\phi$ between the dijet and the dilepton systems), $p_T^{\ell\ell}$, p_T^{jj} , $\min(\Delta R_{j\ell})$, and $m_T = \sqrt{2p_T^{\ell\ell} p_T^{\text{miss}} [1 - \cos \Delta\phi(\ell\ell, \vec{p}_T^{\text{miss}})]}$.

The DNNs utilise a parameterised machine learning technique [74] in order to ensure optimal sensitivity on the full range of signal hypotheses considered in these searches. In this approach, one or more physics parameters describing the wider scope of the problem, as for example the mass of the resonance in the resonant search case, are provided as input to the DNNs, in addition to reconstructed quantities. The parameterised network is able to perform as well as individual networks trained on specific hypotheses (parameter values) while requiring only a single training, and provides a smooth interpolation to cases not seen during the training phase, as shown by Fig. 3. Two parameterised DNNs are trained: one for the resonant and one for the nonresonant search. In the first case, the set of parameters are the masses of the resonance, providing 13 values for the network training ($m_\chi = 260, 270, 300, 350, 400, 450, 500, 550, 600, 650, 750, 800, 900 \text{ GeV}$), and a discrete variable indicating the dilepton flavour channel: same flavour (e^+e^- and $\mu^+\mu^-$) or different flavour ($e^\pm\mu^\mp$). In the second case, the parameters are κ_λ and κ_t , providing 32 combinations of those for the network training ($\kappa_\lambda = -20, -5, 0, 1, 2.4, 3.8, 5, 20$ and $\kappa_t = 0.5, 1, 1.75, 2.5$), and the dilepton flavour channel variable as in the resonant case.

The m_{jj} distributions, and resonant and nonresonant DNN discriminators after selection requirements, are shown in Figs. 4 and 5, respectively. Given their discrimination power between signal and background, both variables are used to enhance the sensitivity of the analysis. We define three regions in m_{jj} : two of them enriched in background, $m_{jj} < 75 \text{ GeV}$ and $m_{jj} \geq 140 \text{ GeV}$, and the other enriched in signal, $m_{jj} \in [75, 140) \text{ GeV}$. In each region, we use the DNN output as our final discriminant, as shown in Fig. 6, where the three m_{jj} regions are represented in a single distribution.

6 Systematic uncertainties

We investigate sources of systematic uncertainties and their impact on the statistical interpretation of the results by considering both uncertainties in the normalisation of the various processes in the analysis, as well as those affecting the shapes of the distributions.

Theoretical uncertainties in the cross sections of backgrounds estimated using simulation are considered as systematic uncertainties in the yield predictions. The uncertainty in the total integrated luminosity is determined to be 2.5% [75].

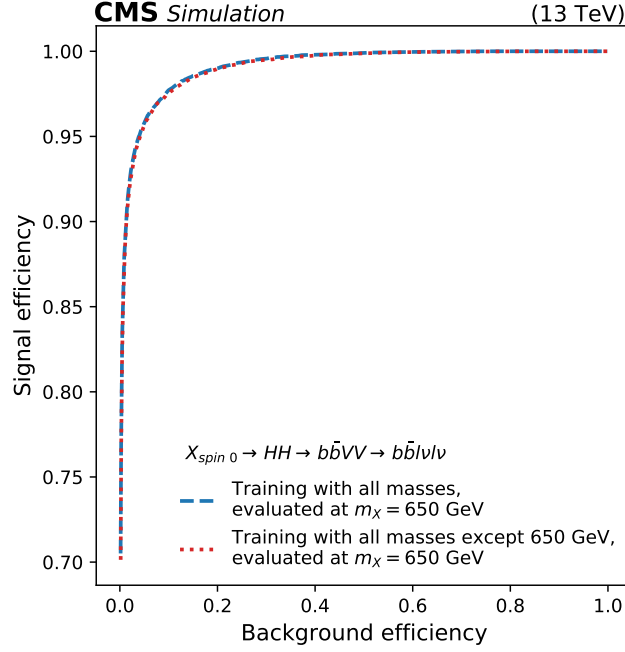


Figure 3: Performance of the parameterised DNN for the resonant search, shown as the selection efficiency for the $m_\chi = 650$ GeV signal as a function of the selection efficiency for the background (ROC curve), for the combined e^+e^- , $\mu^+\mu^-$ and $e^\pm\mu^\mp$ channels. The dashed line corresponds to the DNN used in the analysis, trained on all available signal samples, and evaluated at $m_\chi = 650$ GeV. The dotted line shows an alternative DNN trained using all signal samples except for $m_\chi = 650$ GeV, and evaluated at $m_\chi = 650$ GeV. Both curves overlap, indicating that the parameterised DNN is able to generalise to cases not seen during the training phase by interpolating the signal behaviour from nearby m_χ points.

The following sources of systematic uncertainties that affect the normalisation and shape of the templates used in the statistical evaluation are considered:

- **Trigger efficiency, lepton identification and isolation:** uncertainties in the measurement, using a “tag-and-probe” technique, of trigger efficiencies as well as electron and muon isolation and identification efficiencies, are considered as sources of systematic uncertainties. These are evaluated as a function of lepton p_T and η , and their effect on the analysis is estimated by varying the corrections to the efficiencies by ± 1 standard deviation.
- **Jet energy scale and resolution:** uncertainties in the jet energy scale are of the order of a few percent and are computed as a function of jet p_T and η [67]. A difference in the jet energy resolution of about 10% between data and simulation is accounted for by worsening the jet energy resolution in simulation by η -dependent factors. The uncertainty due to these corrections is estimated by a variation of the factors applied by ± 1 standard deviation. Variations of jet energies are propagated to \vec{p}_T^{miss} .
- **b tagging:** b tagging efficiency and light-flavour mistag rate corrections and associated uncertainties are determined as a function of the jet p_T [71]. Their effect on the analysis is estimated by varying these corrections by ± 1 standard deviation.
- **Pileup:** the measured total inelastic cross section is varied by $\pm 5\%$ [76] to produce different expected pileup distributions.
- **Renormalisation and factorisation scale uncertainty:** this uncertainty is estimated

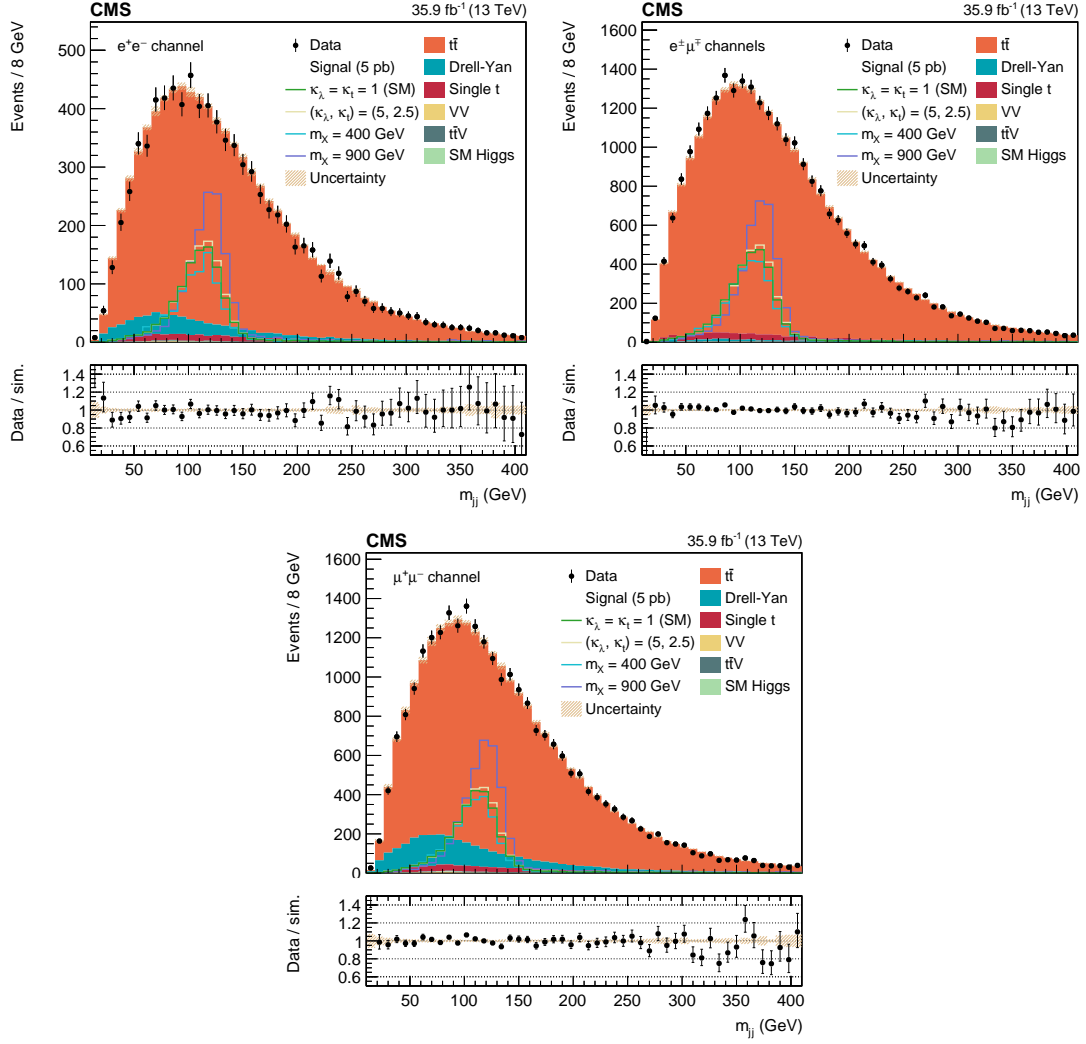


Figure 4: The m_{jj} distribution in data and simulated events after requiring all selection criteria in the e^+e^- (top left), $e^\pm\mu^\mp$ (top right), and $\mu^+\mu^-$ (bottom) channels. The various signal hypotheses displayed have been scaled to a cross section of 5 pb for display purposes. Error bars indicate statistical uncertainties, while shaded bands show post-fit systematic uncertainties.

by varying the renormalisation (μ_R) and the factorisation (μ_F) scales used during the generation of the simulated samples independently by factors of 0.5, 1, or 2. Unphysical cases, where the two scales are at opposite extremes, are not considered. An envelope is built from the 6 possible combinations by keeping maximum and minimum variations for each bin of the distributions, and is used as an estimate of the scale uncertainties for all the background and signal samples.

- **PDF uncertainty:** the magnitudes of the uncertainties related to the PDFs and the variation of the strong coupling constant for each simulated background and signal process are obtained using variations of the NNPDF 3.0 set [54], following the PDF4LHC prescriptions [77, 78].
- **Simulated sample size:** the finite nature of simulated samples is considered as an additional source of systematic uncertainty. For each bin of the distributions, one additional uncertainty is added, where only the considered bin is altered by ± 1 standard deviation, keeping the others at their nominal value.

- **DY background estimate from data:** the systematic uncertainties listed above, which affect the simulation samples, are propagated to ϵ_k and F_{kl} , both computed from simulation. These uncertainties are then propagated to the weights W_{sim} and to the normalisation and shape of the estimated DY background contribution. The uncertainty due to the finite size of the simulation samples used for the determination of ϵ_k and F_{kl} is also taken into account. Since previous measurements [79, 80] have shown that the flavour composition of DY events with associated jets in data is compatible with the simulation within scale uncertainties, no extra source of theoretical uncertainty has been considered for F_{kl} . To account for residual differences between the e^+e^- and $\mu^+\mu^-$ channels not taken into account by F_{kl} , due to the different requirements on lepton p_T , a 5% uncertainty in the normalisation of the DY background estimate is added in both channels.

The effects of these uncertainties on the total yields in the analysis selection are summarised in Table 1.

7 Results

A binned maximum likelihood fit is performed in order to extract best fit signal cross sections. The fit is performed using templates built from the DNN output distributions in the three m_{jj} regions, as shown in Fig. 6, and in the three channels (e^+e^- , $\mu^+\mu^-$, and $e^\pm\mu^\mp$). The likelihood function is the product of the Poisson likelihoods over all bins of the templates and is given by

$$L(\beta_{\text{signal}}, \beta_k | \text{data}) = \prod_{i=1}^{N_{\text{bins}}} \frac{\mu_i^{n_i} e^{-\mu_i}}{n_i!},$$

where n_i is the number of observed events in bin i and the Poisson mean for bin i is given by

$$\mu_i = \beta_{\text{signal}} S_i + \sum_k \beta_k T_{k,i},$$

where k denotes all of the considered background processes, $T_{k,i}$ is the bin content of bin i of the template for process k , and S_i is the bin content of bin i of the signal template. The parameter β_k is the nuisance parameter for the normalisation of the process k , constrained by theoretical uncertainties with a log-normal prior, and β_{signal} is the signal strength, unconstrained. For each systematic uncertainty affecting the shape (normalisation) of the templates, a nuisance parameter is introduced with a Gaussian (log-normal) prior.

The best-fit values for all the nuisance parameters, as well as the corresponding post-fit uncertainties, are extracted by performing a binned maximum likelihood fit, in the background-only hypothesis, of the m_{jj} vs. DNN output distributions (such as Fig. 6 left) to the data. Only nuisance parameters affecting the backgrounds are considered.

7.1 Resonant production

The fit results in signal cross sections compatible with zero; no significant excess above background predictions is observed for X particle mass hypotheses between 260 and 900 GeV. We set upper limits at 95% confidence level (CL) on the product of the production cross section for X and branching fraction for $X \rightarrow HH \rightarrow b\bar{b}V\bar{V} \rightarrow b\bar{b}\ell\nu\ell\nu$ using the asymptotic modified frequentist method (asymptotic CL_s) [81–83] as a function of the X mass hypothesis. The limits are shown in Fig. 7. The observed upper limits on the product of the production cross section and branching fraction for a narrow-width spin-0 resonance range from 430 to 17 fb, in agreement

Table 1: Summary of the systematic uncertainties and their impact on total background yields and on the SM and $m_\chi = 400$ GeV signal hypotheses in the signal region.

Source	Background yield variation	Signal yield variation
Electron identification and isolation	2.0–3.2%	1.9–2.9%
Jet b tagging (heavy-flavour jets)	2.5%	2.5–2.7%
Integrated luminosity	2.5%	2.5%
Trigger efficiency	0.5–1.4%	0.4–1.4%
Pileup	0.3–1.4%	0.3–1.5%
Muon identification	0.4–0.8%	0.4–0.7%
PDFs	0.6–0.7%	1.0–1.4%
Jet b tagging (light-flavour jets)	0.3%	0.3–0.4%
Muon isolation	0.2–0.3%	0.1–0.2%
Jet energy scale	<0.1–0.3%	0.7–1.0%
Jet energy resolution	0.1%	<0.1%
Affecting only $t\bar{t}$ (85.1–95.7% of the total bkg.)		
μ_R and μ_F scales	12.8–12.9%	
$t\bar{t}$ cross section	5.2%	
Simulated sample size	<0.1%	
Affecting only DY in $e^\pm\mu^\mp$ channel (0.9% of the total bkg.)		
μ_R and μ_F scales	24.6–24.7%	
Simulated sample size	7.7–11.6%	
DY cross section	4.9%	
Affecting only DY estimate from data in same-flavour events (7.1–10.7% of the total bkg.)		
Simulated sample size	18.8–19.0%	
Normalisation	5.0%	
Affecting only single top quark (2.5–2.9% of the total bkg.)		
Single t cross section	7.0%	
Simulated sample size	<0.1–1.0%	
μ_R and μ_F scales	<0.1–0.2%	
Affecting only signal	SM signal	$m_\chi = 400$ GeV
μ_R and μ_F scales	24.2%	4.6–4.7%
Simulated sample size	<0.1%	<0.1%

with expected upper limits of 340_{-100}^{+140} to 14_{-4}^{+6} fb. For narrow-width spin-2 particles produced in gluon fusion with minimal gravity-like coupling, the observed upper limits range from 450 to 14 fb, in agreement with expected upper limits of 360_{-100}^{+140} to 13_{-4}^{+6} fb.

The left plot of Fig. 7 shows possible cross sections for the production of a radion, for the parameters $\Lambda_R = 1$ TeV (mass scale) and $kL = 35$ (size of the extra dimension). The right plot of Fig. 7 shows possible cross sections for the production of a Kaluza–Klein graviton, for the parameters $k/\overline{M}_{\text{Pl}} = 0.1$ (curvature) and $kL = 35$. These cross sections are taken from [49], assuming absence of mixing with the Higgs boson.

7.2 Nonresonant production

Likewise for the nonresonant case, the fit results in signal cross sections compatible with zero; no significant excess above background predictions is seen. We set upper limits at 95% CL on the product of the Higgs boson pair production cross section and branching fraction for $HH \rightarrow b\bar{b}VV \rightarrow b\bar{b}\ell\nu\ell\nu$ using the asymptotic CL_s, combining the e^+e^- , $\mu^+\mu^-$ and $e^\pm\mu^\mp$ channels. The observed upper limit on the SM $HH \rightarrow b\bar{b}VV \rightarrow b\bar{b}\ell\nu\ell\nu$ cross section is found to be 72 fb, in agreement with an expected upper limit of 81^{+42}_{-25} fb. Including theoretical uncertainties in the SM signal cross section, this observed upper limit amounts to 79 times the SM prediction, in agreement with an expected upper limit of 89^{+47}_{-28} times the SM prediction.

In the BSM hypothesis, upper limits are set as a function of κ_λ/κ_t , as shown in Fig. 8 (left panel), since the signal kinematics depend only on this ratio of couplings. Red lines show the theoretical cross sections, along with their uncertainties, for $\kappa_t = 1$ (SM) and $\kappa_t = 2$. The theoretical signal cross section is minimal for $\kappa_\lambda/\kappa_t = 2.45$ [84], corresponding to a maximal interference between the diagrams shown on Fig. 1.

Excluded regions in the κ_t vs. κ_λ plane are shown in Fig. 8 (right panel). The signal cross sections and kinematics are invariant under a $(\kappa_\lambda, \kappa_t) \leftrightarrow (-\kappa_\lambda, -\kappa_t)$ transformation, hence the expected and observed limits on the production cross section, as well as the constraints on the κ_λ and κ_t parameters respect the same symmetry. The red region in the panel corresponds to parameters excluded at 95% CL with the observed data, whereas the dashed black line and the blue areas correspond to the expected exclusions and the 68 and 95% bands. Isolines of the product of the theoretical cross section and branching fraction for $HH \rightarrow b\bar{b}VV \rightarrow b\bar{b}\ell\nu\ell\nu$ are shown as dashed-dotted lines.

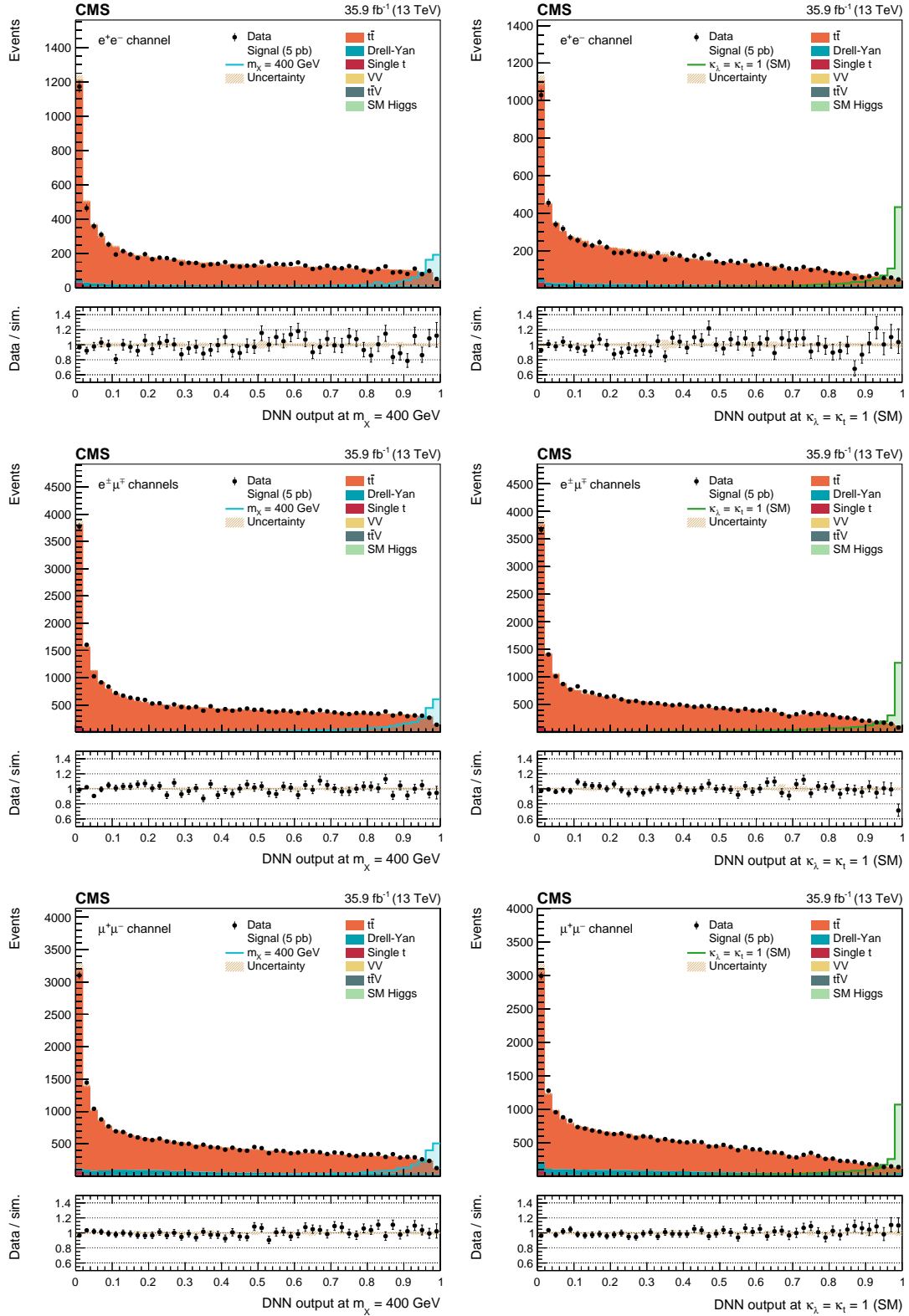


Figure 5: The DNN output distributions in data and simulated events after requiring all selection criteria, in the e^+e^- (top), $e^\pm\mu^\mp$ (middle), and $\mu^+\mu^-$ (bottom) channels. Output values towards 0 are background-like, while output values towards 1 are signal-like. The parameterised resonant DNN output (left) is evaluated at $m_\chi = 400$ GeV and the parameterised nonresonant DNN output (right) is evaluated at $\kappa_\lambda = 1$, $\kappa_t = 1$. The two signal hypotheses displayed have been scaled to a cross section of 5 pb for display purposes. Error bars indicate statistical uncertainties, while shaded bands show post-fit systematic uncertainties.

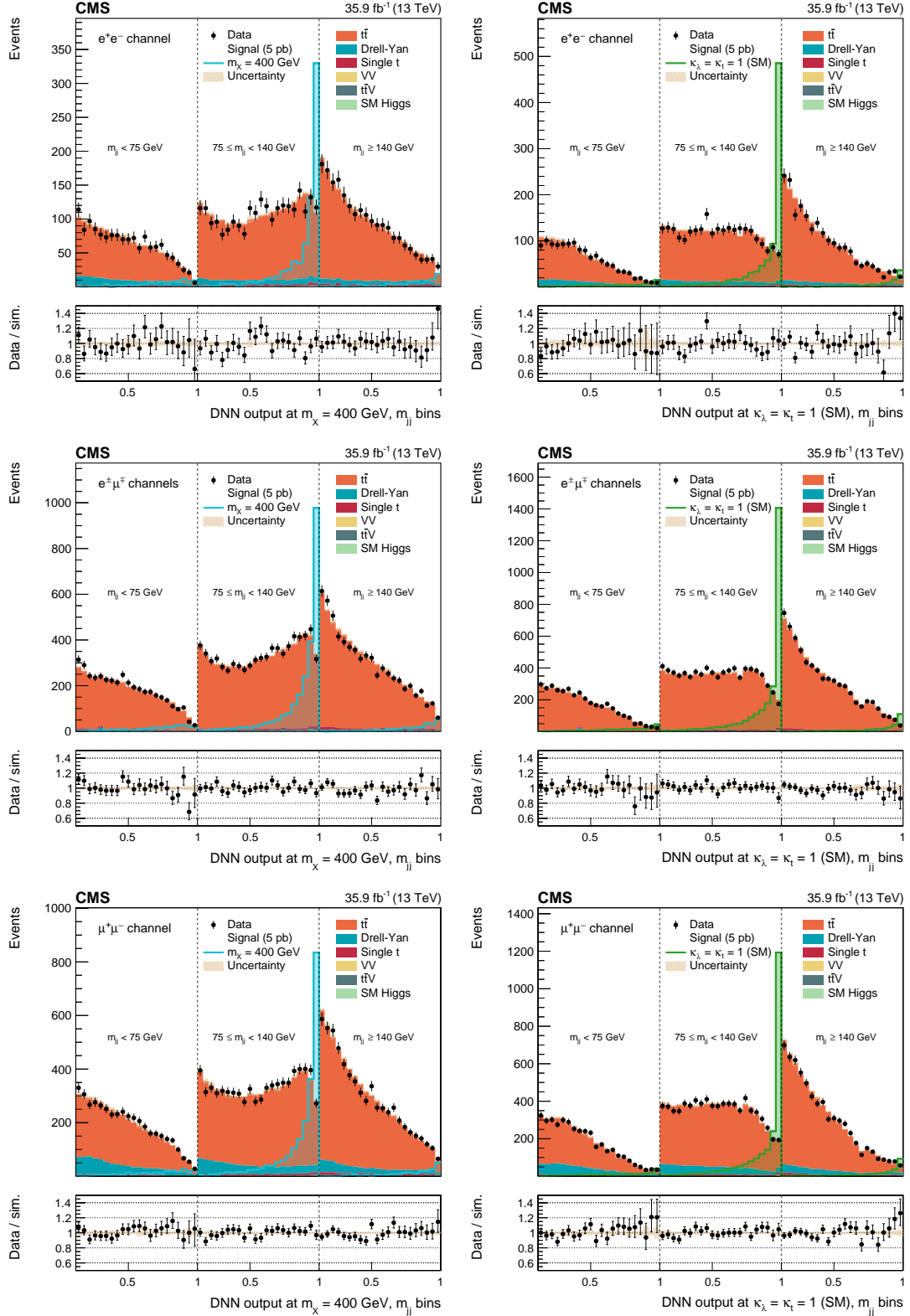


Figure 6: The DNN output distributions in data and simulated events, for the e^+e^- (top), $e^\pm\mu^\mp$ (middle), and $\mu^+\mu^-$ (bottom) channels, in three different m_{jj} regions: $m_{jj} < 75$ GeV, $m_{jj} \in [75, 140)$ GeV, and $m_{jj} \geq 140$ GeV. The parameterised resonant DNN output (left) is evaluated at $m_\chi = 400$ GeV and the parameterised nonresonant DNN output (right) is evaluated at $\kappa_\lambda = \kappa_t = 1$. The two signal hypotheses displayed have been scaled to a cross section of 5 pb for display purposes. Error bars indicate statistical uncertainties, while shaded bands show post-fit systematic uncertainties.

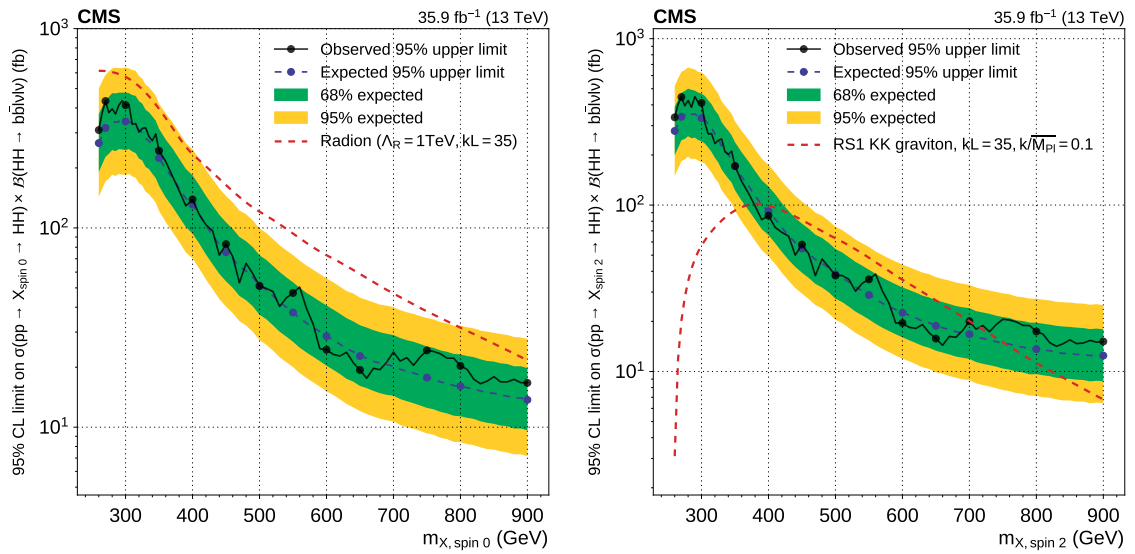


Figure 7: Expected (dashed) and observed (continuous) 95% CL upper limits on the product of the production cross section for $X \rightarrow HH \rightarrow b\bar{b}V\bar{V} \rightarrow b\bar{b}\ell\nu\ell\nu$, as a function of m_X . The inner (green) band and the outer (yellow) band indicate the regions containing 68 and 95%, respectively, of the distribution of limits expected under the background-only hypothesis. These limits are computed using the asymptotic CL_s method, combining the e^+e^- , $\mu^+\mu^-$ and $e^\pm\mu^\mp$ channels, for spin-0 (left) and spin-2 (right) hypotheses. The solid circles represent fully-simulated mass points. The dashed red lines represent possible cross sections for the production of a radion (left) or a Kaluza–Klein graviton (right), assuming absence of mixing with the Higgs boson [49]. Parameters used to compute these cross sections can be found in the legend.

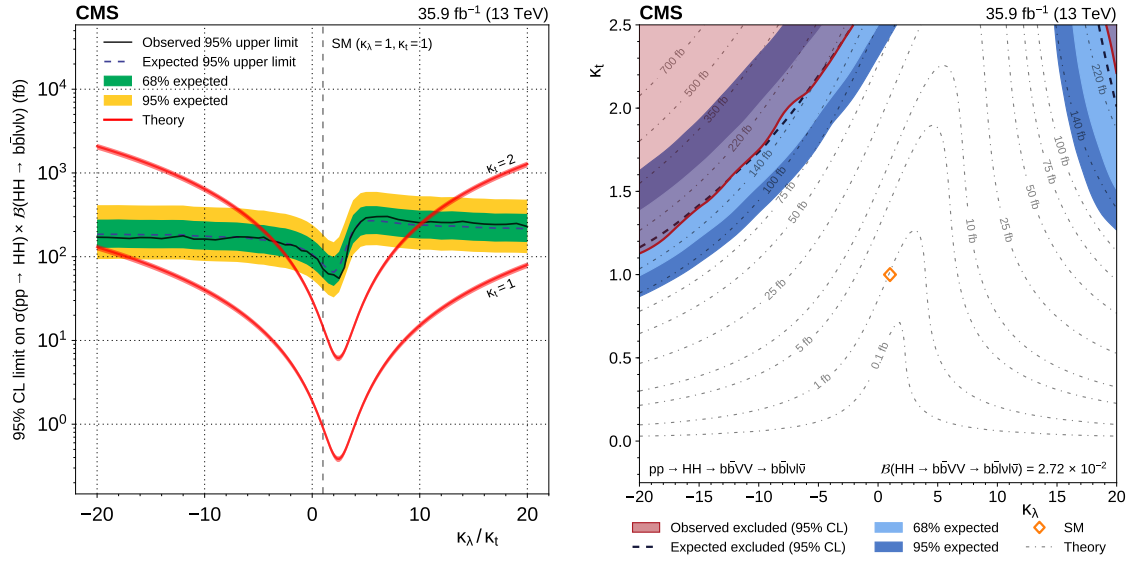


Figure 8: Left: expected (dashed) and observed (continuous) 95% CL upper limits on the product of the Higgs boson pair production cross section and branching fraction for $HH \rightarrow b\bar{b}V\bar{V} \rightarrow b\bar{b}l\nu l\nu$ as a function of $\kappa_\lambda / \kappa_t$. The inner (green) band and the outer (yellow) band indicate the regions containing 68 and 95%, respectively, of the distribution of limits expected under the background-only hypothesis. Red lines show the theoretical cross sections, along with their uncertainties, for $\kappa_t = 1$ (SM) and $\kappa_t = 2$. Right: exclusions in the $(\kappa_\lambda, \kappa_t)$ plane. The red region corresponds to parameters excluded at 95% CL with the observed data, whereas the dashed black line and the blue areas correspond to the expected exclusions and the 68 and 95% bands (light and dark respectively). Isolines of the product of the theoretical cross section and branching fraction for $HH \rightarrow b\bar{b}V\bar{V} \rightarrow b\bar{b}l\nu l\nu$ are shown as dashed-dotted lines. The diamond marker indicates the prediction of the SM. All theoretical predictions are extracted from Refs. [12–17, 84].

8 Summary

A search for resonant and nonresonant Higgs boson pair production (HH) is presented, where one of the Higgs bosons decays to $b\bar{b}$, and the other to $VV \rightarrow \ell\nu\ell\nu$, where V is either a W or a Z boson. The LHC proton-proton collision data at $\sqrt{s} = 13$ TeV collected by the CMS experiment corresponding to an integrated luminosity of 35.9 fb^{-1} are used. Masses are considered in the range between 260 and 900 GeV for the resonant search, while anomalous Higgs boson self-coupling and coupling to the top quark are considered in addition to the standard model case for the nonresonant search.

The results obtained are in agreement, within uncertainties, with the predictions of the standard model. For the resonant search, the data exclude a product of the production cross section and branching fraction of narrow-width spin-0 particles from 430 to 17 fb, in agreement with the expectations of 340^{+140}_{-100} to 14^{+6}_{-4} fb, and narrow-width spin-2 particles produced with minimal gravity-like coupling from 450 to 14 fb, in agreement with the expectations of 360^{+140}_{-100} to 13^{+6}_{-4} fb. For the standard model HH hypothesis, the data exclude a product of the production cross section and branching fraction of 72 fb, corresponding to 79 times the SM cross section. The expected exclusion is 81^{+42}_{-25} fb, corresponding to 89^{+47}_{-28} times the SM cross section.

Acknowledgments

We congratulate our colleagues in the CERN accelerator departments for the excellent performance of the LHC and thank the technical and administrative staffs at CERN and at other CMS institutes for their contributions to the success of the CMS effort. In addition, we gratefully acknowledge the computing centres and personnel of the Worldwide LHC Computing Grid for delivering so effectively the computing infrastructure essential to our analyses. Finally, we acknowledge the enduring support for the construction and operation of the LHC and the CMS detector provided by the following funding agencies: BMWFW and FWF (Austria); FNRS and FWO (Belgium); CNPq, CAPES, FAPERJ, and FAPESP (Brazil); MES (Bulgaria); CERN; CAS, MoST, and NSFC (China); COLCIENCIAS (Colombia); MSES and CSF (Croatia); RPF (Cyprus); SENESCYT (Ecuador); MoER, ERC IUT, and ERDF (Estonia); Academy of Finland, MEC, and HIP (Finland); CEA and CNRS/IN2P3 (France); BMBF, DFG, and HGF (Germany); GSRT (Greece); OTKA and NIH (Hungary); DAE and DST (India); IPM (Iran); SFI (Ireland); INFN (Italy); MSIP and NRF (Republic of Korea); LAS (Lithuania); MOE and UM (Malaysia); BUAP, CINVESTAV, CONACYT, LNS, SEP, and UASLP-FAI (Mexico); MBIE (New Zealand); PAEC (Pakistan); MSHE and NSC (Poland); FCT (Portugal); JINR (Dubna); MON, RosAtom, RAS, RFBR and RAEP (Russia); MESTD (Serbia); SEIDI, CPAN, PCTI and FEDER (Spain); Swiss Funding Agencies (Switzerland); MST (Taipei); ThEPCenter, IPST, STAR, and NSTDA (Thailand); TUBITAK and TAEK (Turkey); NASU and SFFR (Ukraine); STFC (United Kingdom); DOE and NSF (USA).

Individuals have received support from the Marie-Curie programme and the European Research Council and Horizon 2020 Grant, contract No. 675440 (European Union); the Leventis Foundation; the A. P. Sloan Foundation; the Alexander von Humboldt Foundation; the Belgian Federal Science Policy Office; the Fonds pour la Formation à la Recherche dans l'Industrie et dans l'Agriculture (FRIA-Belgium); the Agentschap voor Innovatie door Wetenschap en Technologie (IWT-Belgium); the Ministry of Education, Youth and Sports (MEYS) of the Czech Republic; the Council of Science and Industrial Research, India; the HOMING PLUS programme of the Foundation for Polish Science, cofinanced from European Union, Regional Development Fund, the Mobility Plus programme of the Ministry of Science and Higher Education, the National Science Center (Poland), contracts Harmonia 2014/14/M/ST2/00428, Opus 2014/13/B/ST2/02543, 2014/15/B/ST2/03998, and 2015/19/B/ST2/02861, Sonata-bis 2012/07/E/ST2/01406; the National Priorities Research Program by Qatar National Research Fund; the Programa Clarín-COFUND del Principado de Asturias; the Thalís and Aristeia programmes cofinanced by EU-ESF and the Greek NSRF; the Rachadapisek Sompot Fund for Postdoctoral Fellowship, Chulalongkorn University and the Chulalongkorn Academic into Its 2nd Century Project Advancement Project (Thailand); and the Welch Foundation, contract C-1845.

References

- [1] F. Englert and R. Brout, "Broken Symmetry and the Mass of Gauge Vector Mesons", *Phys. Rev. Lett.* **13** (1964) 321, doi:10.1103/PhysRevLett.13.321.
- [2] P. W. Higgs, "Broken symmetries, massless particles and gauge fields", *Phys. Lett.* **12** (1964) 132, doi:10.1016/0031-9163(64)91136-9.
- [3] P. W. Higgs, "Broken Symmetries and the Masses of Gauge Bosons", *Phys. Rev. Lett.* **13** (1964) 508, doi:10.1103/PhysRevLett.13.508.

- [4] G. S. Guralnik, C. R. Hagen, and T. W. B. Kibble, “Global conservation laws and massless particles”, *Phys. Rev. Lett.* **13** (1964) 585, doi:10.1103/PhysRevLett.13.585.
- [5] P. W. Higgs, “Spontaneous symmetry breakdown without massless bosons”, *Phys. Rev.* **145** (1966) 1156, doi:10.1103/PhysRev.145.1156.
- [6] T. W. B. Kibble, “Symmetry breaking in non-abelian gauge theories”, *Phys. Rev.* **155** (1967) 1554, doi:10.1103/PhysRev.155.1554.
- [7] ATLAS Collaboration, “Observation of a new particle in the search for the Standard Model Higgs boson with the ATLAS detector at the LHC”, *Phys. Lett. B* **716** (2012) 1, doi:10.1016/j.physletb.2012.08.020, arXiv:1207.7214.
- [8] CMS Collaboration, “Observation of a new boson at a mass of 125 GeV with the CMS experiment at the LHC”, *Phys. Lett. B* **716** (2012) 30, doi:10.1016/j.physletb.2012.08.021, arXiv:1207.7235.
- [9] CMS Collaboration, “Observation of a new boson with mass near 125 GeV in pp collisions at $\sqrt{s} = 7$ and 8 TeV”, *JHEP* **06** (2013) 081, doi:10.1007/JHEP06(2013)081, arXiv:1303.4571.
- [10] CMS Collaboration, “Higgs pair production at the High Luminosity LHC”, CMS Physics Analysis Summary CMS-PAS-FTR-15-002, 2015.
- [11] CMS Collaboration, “Projected performance of Higgs analyses at the HL-LHC for ECFA 2016”, CMS Physics Analysis Summary CMS-PAS-FTR-16-002, 2017.
- [12] D. de Florian et al., “Handbook of LHC Higgs cross sections: 4. deciphering the nature of the Higgs sector”, CERN Yellow Report CERN-2017-002-M, 2016. doi:10.23731/CYRM-2017-002, arXiv:1610.07922.
- [13] D. de Florian and J. Mazzitelli, “Higgs pair production at next-to-next-to-leading logarithmic accuracy at the LHC”, *JHEP* **09** (2015) 053, doi:10.1007/JHEP09(2015)053, arXiv:1505.07122.
- [14] D. de Florian and J. Mazzitelli, “Higgs boson pair production at next-to-next-to-leading order in QCD”, *Phys. Rev. Lett.* **111** (2013) 201801, doi:10.1103/PhysRevLett.111.201801, arXiv:1309.6594.
- [15] S. Borowka et al., “Higgs boson pair production in gluon fusion at next-to-leading order with full top-quark mass dependence”, *Phys. Rev. Lett.* **117** (2016) 012001, doi:10.1103/PhysRevLett.117.012001, arXiv:1604.06447. [Erratum: doi:10.1103/PhysRevLett.117.079901].
- [16] S. Dawson, S. Dittmaier, and M. Spira, “Neutral Higgs-boson pair production at hadron colliders: QCD corrections”, *Phys. Rev. D* **58** (1998) 115012, doi:10.1103/PhysRevD.58.115012, arXiv:hep-ph/9805244.
- [17] J. Grigo, K. Melnikov, and M. Steinhauser, “Virtual corrections to Higgs boson pair production in the large top quark mass limit”, *Nucl. Phys. B* **888** (2014) 17, doi:10.1016/j.nuclphysb.2014.09.003, arXiv:1408.2422.
- [18] J. Grigo, J. Hoff, and M. Steinhauser, “Higgs boson pair production: Top quark mass effects at NLO and NNLO”, *Nucl. Phys. B* **900** (2015) 412, doi:10.1016/j.nuclphysb.2015.09.012, arXiv:1508.00909.

- [19] J. Grigo, J. Hoff, K. Melnikov, and M. Steinhauser, “On the Higgs boson pair production at the LHC”, *Nucl. Phys. B* **875** (2013) 1, doi:10.1016/j.nuclphysb.2013.06.024, arXiv:1305.7340.
- [20] R. Frederix et al., “Higgs pair production at the LHC with NLO and parton-shower effects”, *Phys. Lett. B* **732** (2014) 142, doi:10.1016/j.physletb.2014.03.026, arXiv:1401.7340.
- [21] F. Maltoni, E. Vryonidou, and M. Zaro, “Top-quark mass effects in double and triple Higgs production in gluon-gluon fusion at NLO”, *JHEP* **11** (2014) 079, doi:10.1007/JHEP11(2014)079, arXiv:1408.6542.
- [22] A. Azatov, R. Contino, G. Panico, and M. Son, “Effective field theory analysis of double Higgs boson production via gluon fusion”, *Phys. Rev. D* **92** (2015) 035001, doi:10.1103/PhysRevD.92.035001, arXiv:1502.00539.
- [23] F. Goertz, A. Papaefstathiou, L. L. Yang, and J. Zurita, “Higgs boson pair production in the $D = 6$ extension of the SM”, *JHEP* **04** (2015) 167, doi:10.1007/JHEP04(2015)167, arXiv:1410.3471.
- [24] B. Hespel, D. Lopez-Val, and E. Vryonidou, “Higgs pair production via gluon fusion in the Two-Higgs-Doublet Model”, *JHEP* **09** (2014) 124, doi:10.1007/JHEP09(2014)124, arXiv:1407.0281.
- [25] G. C. Branco et al., “Theory and phenomenology of two-Higgs-doublet models”, *Phys. Rept.* **516** (2012) 1, doi:10.1016/j.physrep.2012.02.002, arXiv:1106.0034.
- [26] L. Randall and R. Sundrum, “A large mass hierarchy from a small extra dimension”, *Phys. Rev. Lett.* **83** (1999) 3370, doi:10.1103/PhysRevLett.83.3370, arXiv:hep-ph/9905221.
- [27] W. D. Goldberger and M. S. Wise, “Modulus stabilization with bulk fields”, *Phys. Rev. Lett.* **83** (1999) 4922, doi:10.1103/PhysRevLett.83.4922, arXiv:hep-ph/9907447.
- [28] O. DeWolfe, D. Freedman, S. Gubser, and A. Karch, “Modeling the fifth dimension with scalars and gravity”, *Phys. Rev. D* **62** (2000) 046008, doi:10.1103/PhysRevD.62.046008, arXiv:hep-th/9909134.
- [29] C. Csaki, M. Graesser, L. Randall, and J. Terning, “Cosmology of brane models with radion stabilization”, *Phys. Rev. D* **62** (2000) 045015, doi:10.1103/PhysRevD.62.045015, arXiv:hep-ph/9911406.
- [30] C. Csaki, J. Hubisz, and S. J. Lee, “Radion phenomenology in realistic warped space models”, *Phys. Rev. D* **76** (2007) 125015, doi:10.1103/PhysRevD.76.125015, arXiv:0705.3844.
- [31] H. Davoudiasl, J. Hewett, and T. Rizzo, “Phenomenology of the Randall-Sundrum gauge hierarchy model”, *Phys. Rev. Lett.* **84** (2000) 2080, doi:10.1103/PhysRevLett.84.2080, arXiv:hep-ph/9909255.
- [32] C. Csaki, M. L. Graesser, and G. D. Kribs, “Radion dynamics and electroweak physics”, *Phys. Rev. D* **63** (2001) 065002, doi:10.1103/PhysRevD.63.065002, arXiv:hep-th/0008151.

- [33] CMS Collaboration, “Search for two Higgs bosons in final states containing two photons and two bottom quarks in proton-proton collisions at 8 TeV”, *Phys. Rev. D* **94** (2016) 052012, doi:10.1103/PhysRevD.94.052012, arXiv:1603.06896.
- [34] ATLAS Collaboration, “Search for Higgs boson pair production in the $\gamma\gamma b\bar{b}$ Final State using pp collision Data at $\sqrt{s} = 8$ TeV from the ATLAS detector”, *Phys. Rev. Lett.* **114** (2015) 081802, doi:10.1103/PhysRevLett.114.081802, arXiv:1406.5053.
- [35] ATLAS Collaboration, “Search for Higgs boson pair production in the $b\bar{b}b\bar{b}$ final state from pp collisions at $\sqrt{s} = 8$ TeV with the ATLAS detector”, *Eur. Phys. J. C* **75** (2015) 412, doi:10.1140/epjc/s10052-015-3628-x, arXiv:1506.00285.
- [36] ATLAS Collaboration, “Searches for Higgs boson pair production in the $hh \rightarrow b\bar{b}\tau\tau, \gamma\gamma WW^*, \gamma\gamma b\bar{b}, b\bar{b}b\bar{b}$ channels with the ATLAS detector”, *Phys. Rev. D* **92** (2015) 092004, doi:10.1103/PhysRevD.92.092004, arXiv:1509.04670.
- [37] CMS Collaboration, “A search for Higgs boson pair production in the $b\bar{b}\tau\tau$ final state in proton-proton collisions at $\sqrt{s} = 8$ TeV”, (2017). arXiv:1707.00350. Submitted to *Phys. Rev. D*.
- [38] ATLAS Collaboration, “Search for pair production of Higgs bosons in the $b\bar{b}b\bar{b}$ final state using proton-proton collisions at $\sqrt{s} = 13$ TeV with the ATLAS detector”, *Phys. Rev. D* **94** (2016) 052002, doi:10.1103/PhysRevD.94.052002, arXiv:1606.04782.
- [39] CMS Collaboration, “Search for Higgs boson pair production in events with two bottom quarks and two tau leptons in proton-proton collisions at $\sqrt{s} = 13$ TeV”, (2017). arXiv:1707.02909. Submitted to *Phys. Lett. B*.
- [40] CMS Collaboration, “The CMS experiment at the CERN LHC”, *JINST* **03** (2008) S08004, doi:10.1088/1748-0221/3/08/S08004.
- [41] P. Nason, “A new method for combining NLO QCD with shower Monte Carlo algorithms”, *JHEP* **11** (2004) 040, doi:10.1088/1126-6708/2004/11/040, arXiv:hep-ph/0409146.
- [42] S. Frixione, P. Nason, and C. Oleari, “Matching NLO QCD computations with parton shower simulations: the POWHEG method”, *JHEP* **11** (2007) 070, doi:10.1088/1126-6708/2007/11/070, arXiv:0709.2092.
- [43] S. Alioli, P. Nason, C. Oleari, and E. Re, “A general framework for implementing NLO calculations in shower Monte Carlo programs: the POWHEG BOX”, *JHEP* **06** (2010) 043, doi:10.1007/JHEP06(2010)043, arXiv:1002.2581.
- [44] S. Alioli, S. O. Moch, and P. Uwer, “Hadronic top-quark pair-production with one jet and parton showering”, *JHEP* **01** (2012) 137, doi:10.1007/JHEP01(2012)137, arXiv:1110.5251.
- [45] S. Alioli, P. Nason, C. Oleari, and E. Re, “NLO single-top production matched with shower in POWHEG: s - and t -channel contributions”, *JHEP* **09** (2009) 111, doi:10.1088/1126-6708/2009/09/111, arXiv:0907.4076. [Erratum: doi:10.1007/JHEP02(2010)011].
- [46] J. Alwall et al., “The automated computation of tree-level and next-to-leading order differential cross sections, and their matching to parton shower simulations”, *JHEP* **07** (2014) 079, doi:10.1007/JHEP07(2014)079, arXiv:1405.0301.

- [47] R. Frederix and S. Frixione, “Merging meets matching in MC@NLO”, *JHEP* **12** (2012) 061, doi:10.1007/JHEP12(2012)061, arXiv:1209.6215.
- [48] P. Artoisenet, R. Frederix, O. Mattelaer, and R. Rietkerk, “Automatic spin-entangled decays of heavy resonances in Monte Carlo simulations”, *JHEP* **03** (2013) 015, doi:10.1007/JHEP03(2013)015, arXiv:1212.3460.
- [49] A. Oliveira, “Gravity particles from warped extra dimensions, predictions for LHC”, arXiv:1404.0102.
- [50] C. C. ATLAS, “Combined Measurement of the Higgs Boson Mass in pp Collisions at $\sqrt{s} = 7$ and 8 TeV with the ATLAS and CMS Experiments”, *Phys. Rev. Lett.* **114** (2015) 191803, doi:10.1103/PhysRevLett.114.191803, arXiv:1503.07589.
- [51] T. Sjöstrand, S. Mrenna, and P. Z. Skands, “PYTHIA 6.4 physics and manual”, *JHEP* **05** (2006) 026, doi:10.1088/1126-6708/2006/05/026, arXiv:hep-ph/0603175.
- [52] T. Sjöstrand, S. Mrenna, and P. Z. Skands, “A brief introduction to PYTHIA 8.1”, *Comput. Phys. Commun.* **178** (2008) 852, doi:10.1016/j.cpc.2008.01.036, arXiv:0710.3820.
- [53] CMS Collaboration, “Event generator tunes obtained from underlying event and multiparton scattering measurements”, *Eur. Phys. J. C* **76** (2015) 155, doi:10.1140/epjc/s10052-016-3988-x, arXiv:1512.00815.
- [54] NNPDF Collaboration, “Parton distributions for the LHC Run II”, *JHEP* **04** (2015) 040, doi:10.1007/JHEP04(2015)040, arXiv:1410.8849.
- [55] GEANT4 Collaboration, “GEANT4—a simulation toolkit”, *Nucl. Instrum. Meth. A* **506** (2003) 250, doi:10.1016/S0168-9002(03)01368-8.
- [56] M. Czakon and A. Mitov, “Top++: A program for the calculation of the top-pair cross-section at hadron colliders”, *Comput. Phys. Commun.* **185** (2014) 2930, doi:10.1016/j.cpc.2014.06.021, arXiv:1112.5675.
- [57] Y. Li and F. Petriello, “Combining QCD and electroweak corrections to dilepton production in the framework of the FEWZ simulation code”, *Phys. Rev. D* **86** (2012) 094034, doi:10.1103/PhysRevD.86.094034, arXiv:1208.5967.
- [58] N. Kidonakis, “Top Quark Production”, arXiv:1311.0283.
- [59] T. Gehrmann et al., “ W^+W^- production at hadron colliders in next to next to leading order QCD”, *Phys. Rev. Lett.* **113** (2014) 212001, doi:10.1103/PhysRevLett.113.212001, arXiv:1408.5243.
- [60] J. M. Campbell, R. K. Ellis, and C. Williams, “Vector boson pair production at the LHC”, *JHEP* **07** (2011) 018, doi:10.1007/JHEP07(2011)018, arXiv:1105.0020.
- [61] CMS Collaboration, “Measurement of the inclusive W and Z production cross sections in pp collisions at $\sqrt{s} = 7$ TeV with the CMS experiment”, *JHEP* **10** (2011) 132, doi:10.1007/JHEP10(2011)132, arXiv:1107.4789.
- [62] CMS Collaboration, “Performance of electron reconstruction and selection with the CMS detector in proton-proton collisions at $\sqrt{s} = 8$ TeV”, *JINST* **10** (2015) P06005, doi:10.1088/1748-0221/10/06/P06005, arXiv:1502.02701.

- [63] CMS Collaboration, “Performance of CMS muon reconstruction in pp collision events at $\sqrt{s} = 7$ TeV”, *JINST* **7** (2012) P10002, doi:10.1088/1748-0221/7/10/P10002, arXiv:1206.4071.
- [64] CMS Collaboration, “Particle-flow reconstruction and global event description with the CMS detector”, *JINST* **12** (2017) P10003, doi:10.1088/1748-0221/12/10/P10003, arXiv:1706.04965.
- [65] M. Cacciari, G. P. Salam, and G. Soyez, “The anti- k_T jet clustering algorithm”, *JHEP* **04** (2008) 063, doi:10.1088/1126-6708/2008/04/063, arXiv:0802.1189.
- [66] M. Cacciari, G. P. Salam, and G. Soyez, “FastJet user manual”, *Eur. Phys. J. C* **72** (2012) 1896, doi:10.1140/epjc/s10052-012-1896-2, arXiv:1111.6097.
- [67] CMS Collaboration, “Jet energy scale and resolution in the CMS experiment in pp collisions at 8 TeV”, *JINST* **12** (2017) P02014, doi:10.1088/1748-0221/12/02/P02014, arXiv:1607.03663.
- [68] CMS Collaboration, “Performance of the CMS missing transverse momentum reconstruction in pp data at $\sqrt{s} = 8$ TeV”, *JINST* **10** (2015) P02006, doi:10.1088/1748-0221/10/02/P02006, arXiv:1411.0511.
- [69] CMS Collaboration, “Performance of missing energy reconstruction in 13 TeV pp collision data using the CMS detector”, CMS Physics Analysis Summary CMS-PAS-JME-16-004, 2016.
- [70] CMS Collaboration, “Identification of b-quark jets with the CMS experiment”, *JINST* **8** (2013) P04013, doi:10.1088/1748-0221/8/04/P04013, arXiv:1211.4462.
- [71] CMS Collaboration, “Identification of b quark jets at the CMS Experiment in the LHC Run 2”, CMS Physics Analysis Summary CMS-PAS-BTV-15-001, 2016.
- [72] H. Voss, A. Höcker, J. Stelzer, and F. Tegenfeldt, “TMVA, the toolkit for multivariate data analysis with ROOT”, in *XIth International Workshop on Advanced Computing and Analysis Techniques in Physics Research (ACAT)*, p. 40. 2007. arXiv:physics/0703039.
- [73] F. Chollet, “keras”. <https://github.com/fchollet/keras>, 2015.
- [74] P. Baldi et al., “Parameterized neural networks for high-energy physics”, *Eur. Phys. J. C* **76** (2016) 235, doi:10.1140/epjc/s10052-016-4099-4, arXiv:1601.07913.
- [75] CMS Collaboration, “CMS Luminosity Measurements for the 2016 Data Taking Period”, CMS Physics Analysis Summary CMS-PAS-LUM-17-001, 2017.
- [76] ATLAS Collaboration, “Measurement of the Inelastic Proton-Proton Cross Section at $\sqrt{s} = 13$ TeV with the ATLAS Detector at the LHC”, *Phys. Rev. Lett.* **117** (2016) 182002, doi:10.1103/PhysRevLett.117.182002, arXiv:1606.02625.
- [77] M. Botje et al., “The PDF4LHC Working Group interim recommendations”, 2011. arXiv:1101.0538.
- [78] S. Alekhin et al., “The PDF4LHC Working Group interim report”, 2011. arXiv:1101.0536.

- [79] CMS Collaboration, “Measurement of the production cross sections for a Z boson and one or more b jets in pp collisions at $\sqrt{s} = 7$ TeV”, *JHEP* **06** (2014) 120, doi:10.1007/JHEP06(2014)120, arXiv:1402.1521.
- [80] CMS Collaboration, “Measurements of the associated production of a Z boson and b jets in pp collisions at $\sqrt{s} = 8$ TeV”, (2016). arXiv:1611.06507. Submitted to *Eur. Phys. J. C*.
- [81] T. Junk, “Confidence level computation for combining searches with small statistics”, *Nucl. Instrum. Meth. A* **434** (1999) 435, doi:10.1016/S0168-9002(99)00498-2, arXiv:hep-ex/9902006.
- [82] A. L. Read, “Presentation of search results: the CL_s technique”, *J. Phys. G* **28** (2002) 2693, doi:10.1088/0954-3899/28/10/313.
- [83] G. Cowan, K. Cranmer, E. Gross, and O. Vitells, “Asymptotic formulae for likelihood-based tests of new physics”, *Eur. Phys. J. C* **71** (2011) 1554, doi:10.1140/epjc/s10052-011-1554-0, arXiv:1007.1727. [Erratum: doi:10.1140/epjc/s10052-013-2501-z].
- [84] A. Carvalho et al., “Analytical parametrization and shape classification of anomalous HH production in EFT approach”, LHCHXSWG report, 2016. arXiv:1608.06578.

A The CMS Collaboration

Yerevan Physics Institute, Yerevan, Armenia

A.M. Sirunyan, A. Tumasyan

Institut für Hochenergiephysik, Wien, Austria

W. Adam, F. Ambrogio, E. Asilar, T. Bergauer, J. Brandstetter, E. Brondolin, M. Dragicevic, J. Erö, M. Flechl, M. Friedl, R. Frühwirth¹, V.M. Ghete, J. Grossmann, J. Hrubec, M. Jeitler¹, A. König, N. Krammer, I. Krätschmer, D. Liko, T. Madlener, I. Mikulec, E. Pree, D. Rabady, N. Rad, H. Rohringer, J. Schieck¹, R. Schöfbeck, M. Spanring, D. Spitzbart, W. Waltenberger, J. Wittmann, C.-E. Wulz¹, M. Zarucki

Institute for Nuclear Problems, Minsk, Belarus

V. Chekhovsky, V. Mossolov, J. Suarez Gonzalez

Universiteit Antwerpen, Antwerpen, Belgium

E.A. De Wolf, D. Di Croce, X. Janssen, J. Lauwers, H. Van Haevermaet, P. Van Mechelen, N. Van Remortel

Vrije Universiteit Brussel, Brussel, Belgium

S. Abu Zeid, F. Blekman, J. D'Hondt, I. De Bruyn, J. De Clercq, K. Deroover, G. Flouris, D. Lontkovskyi, S. Lowette, S. Moortgat, L. Moreels, Q. Python, K. Skovpen, S. Tavernier, W. Van Doninck, P. Van Mulders, I. Van Parijs

Université Libre de Bruxelles, Bruxelles, Belgium

H. Brun, B. Clerbaux, G. De Lentdecker, H. Delannoy, G. Fasanella, L. Favart, R. Goldouzian, A. Grebenyuk, G. Karapostoli, T. Lenzi, J. Luetic, T. Maerschalk, A. Marinov, A. Randle-conde, T. Seva, C. Vander Velde, P. Vanlaer, D. Vannerom, R. Yonamine, F. Zenoni, F. Zhang²

Ghent University, Ghent, Belgium

A. Cimmino, T. Cornelis, D. Dobur, A. Fagot, M. Gul, I. Khvastunov, D. Poyraz, C. Roskas, S. Salva, M. Tytgat, W. Verbeke, N. Zaganidis

Université Catholique de Louvain, Louvain-la-Neuve, Belgium

H. Bakhshiansohi, O. Bondu, S. Brochet, G. Bruno, A. Caudron, S. De Visscher, C. Delaere, M. Delcourt, B. Francois, A. Giammanco, A. Jafari, M. Komm, G. Krintiras, V. Lemaitre, A. Magitteri, A. Mertens, M. Musich, K. Piotrkowski, L. Quertenmont, M. Vidal Marono, S. Wertz

Université de Mons, Mons, Belgium

N. Bely

Centro Brasileiro de Pesquisas Fisicas, Rio de Janeiro, Brazil

W.L. Aldá Júnior, F.L. Alves, G.A. Alves, L. Brito, M. Correa Martins Junior, C. Hensel, A. Moraes, M.E. Pol, P. Rebello Teles

Universidade do Estado do Rio de Janeiro, Rio de Janeiro, Brazil

E. Belchior Batista Das Chagas, W. Carvalho, J. Chinellato³, A. Custódio, E.M. Da Costa, G.G. Da Silveira⁴, D. De Jesus Damiao, S. Fonseca De Souza, L.M. Huertas Guativa, H. Malbouisson, M. Melo De Almeida, C. Mora Herrera, L. Mundim, H. Nogima, A. Santoro, A. Sznajder, E.J. Tonelli Manganote³, F. Torres Da Silva De Araujo, A. Vilela Pereira

Universidade Estadual Paulista ^a, Universidade Federal do ABC ^b, São Paulo, Brazil

S. Ahuja^a, C.A. Bernardes^a, T.R. Fernandez Perez Tomei^a, E.M. Gregores^b, P.G. Mercadante^b, S.F. Novaes^a, Sandra S. Padula^a, D. Romero Abad^b, J.C. Ruiz Vargas^a

Institute for Nuclear Research and Nuclear Energy of Bulgaria Academy of Sciences

A. Aleksandrov, R. Hadjiiska, P. Iaydjiev, M. Misheva, M. Rodozov, M. Shopova, S. Stoykova, G. Sultanov

University of Sofia, Sofia, Bulgaria

A. Dimitrov, I. Glushkov, L. Litov, B. Pavlov, P. Petkov

Beihang University, Beijing, China

W. Fang⁵, X. Gao⁵

Institute of High Energy Physics, Beijing, China

M. Ahmad, J.G. Bian, G.M. Chen, H.S. Chen, M. Chen, Y. Chen, C.H. Jiang, D. Leggat, H. Liao, Z. Liu, F. Romeo, S.M. Shaheen, A. Spiezia, J. Tao, C. Wang, Z. Wang, E. Yazgan, H. Zhang, J. Zhao

State Key Laboratory of Nuclear Physics and Technology, Peking University, Beijing, China

Y. Ban, G. Chen, Q. Li, S. Liu, Y. Mao, S.J. Qian, D. Wang, Z. Xu

Universidad de Los Andes, Bogota, Colombia

C. Avila, A. Cabrera, L.F. Chaparro Sierra, C. Florez, C.F. González Hernández, J.D. Ruiz Alvarez

University of Split, Faculty of Electrical Engineering, Mechanical Engineering and Naval Architecture, Split, Croatia

B. Courbon, N. Godinovic, D. Lelas, I. Puljak, P.M. Ribeiro Cipriano, T. Sculac

University of Split, Faculty of Science, Split, Croatia

Z. Antunovic, M. Kovac

Institute Rudjer Boskovic, Zagreb, Croatia

V. Brigljevic, D. Ferencek, K. Kadija, B. Mesic, A. Starodumov⁶, T. Susa

University of Cyprus, Nicosia, Cyprus

M.W. Ather, A. Attikis, G. Mavromanolakis, J. Mousa, C. Nicolaou, F. Ptochos, P.A. Razis, H. Rykaczewski

Charles University, Prague, Czech Republic

M. Finger⁷, M. Finger Jr.⁷

Universidad San Francisco de Quito, Quito, Ecuador

E. Carrera Jarrin

Academy of Scientific Research and Technology of the Arab Republic of Egypt, Egyptian Network of High Energy Physics, Cairo, Egypt

Y. Assran^{8,9}, S. Elgammal⁹, A. Mahrous¹⁰

National Institute of Chemical Physics and Biophysics, Tallinn, Estonia

R.K. Dewanjee, M. Kadastik, L. Perrini, M. Raidal, A. Tiko, C. Veelken

Department of Physics, University of Helsinki, Helsinki, Finland

P. Eerola, J. Pekkanen, M. Voutilainen

Helsinki Institute of Physics, Helsinki, Finland

J. Härkönen, T. Järvinen, V. Karimäki, R. Kinnunen, T. Lampén, K. Lassila-Perini, S. Lehti, T. Lindén, P. Luukka, E. Tuominen, J. Tuominiemi, E. Tuovinen

Lappeenranta University of Technology, Lappeenranta, Finland

J. Talvitie, T. Tuuva

IRFU, CEA, Université Paris-Saclay, Gif-sur-Yvette, France

M. Besancon, F. Couderc, M. Dejardin, D. Denegri, J.L. Faure, F. Ferri, S. Ganjour, S. Ghosh, A. Givernaud, P. Gras, G. Hamel de Monchenault, P. Jarry, I. Kucher, E. Locci, M. Machet, J. Malcles, G. Negro, J. Rander, A. Rosowsky, M.Ö. Sahin, M. Titov

Laboratoire Leprince-Ringuet, Ecole polytechnique, CNRS/IN2P3, Université Paris-Saclay, Palaiseau, France

A. Abdulsalam, I. Antropov, S. Baffioni, F. Beaudette, P. Busson, L. Cadamuro, C. Charlot, R. Granier de Cassagnac, M. Jo, S. Lisniak, A. Lobanov, J. Martin Blanco, M. Nguyen, C. Ochando, G. Ortona, P. Paganini, P. Pigard, S. Regnard, R. Salerno, J.B. Sauvan, Y. Sirois, A.G. Stahl Leiton, T. Strebler, Y. Yilmaz, A. Zabi, A. Zghiche

Université de Strasbourg, CNRS, IPHC UMR 7178, F-67000 Strasbourg, FranceJ.-L. Agram¹¹, J. Andrea, D. Bloch, J.-M. Brom, M. Buttignol, E.C. Chabert, N. Chanon, C. Collard, E. Conte¹¹, X. Coubez, J.-C. Fontaine¹¹, D. Gelé, U. Goerlach, M. Jansová, A.-C. Le Bihan, N. Tonon, P. Van Hove**Centre de Calcul de l'Institut National de Physique Nucleaire et de Physique des Particules, CNRS/IN2P3, Villeurbanne, France**

S. Gadrat

Université de Lyon, Université Claude Bernard Lyon 1, CNRS-IN2P3, Institut de Physique Nucléaire de Lyon, Villeurbanne, FranceS. Beauceron, C. Bernet, G. Boudoul, R. Chierici, D. Contardo, P. Depasse, H. El Mamouni, J. Fay, L. Finco, S. Gascon, M. Gouzevitch, G. Grenier, B. Ille, F. Lagarde, I.B. Laktineh, M. Lethuillier, L. Mirabito, A.L. Pequegnot, S. Perries, A. Popov¹², V. Sordini, M. Vander Donckt, S. Viret**Georgian Technical University, Tbilisi, Georgia**T. Toriashvili¹³**Tbilisi State University, Tbilisi, Georgia**Z. Tsamalaidze⁷**RWTH Aachen University, I. Physikalisches Institut, Aachen, Germany**

C. Autermann, S. Beranek, L. Feld, M.K. Kiesel, K. Klein, M. Lipinski, M. Preuten, C. Schomakers, J. Schulz, T. Verlage

RWTH Aachen University, III. Physikalisches Institut A, Aachen, Germany

A. Albert, E. Dietz-Laursonn, D. Duchardt, M. Endres, M. Erdmann, S. Erdweg, T. Esch, R. Fischer, A. Güth, M. Hamer, T. Hebbeker, C. Heidemann, K. Hoepfner, S. Knutzen, M. Merschmeyer, A. Meyer, P. Millet, S. Mukherjee, M. Olschewski, K. Padeken, T. Pook, M. Radziej, H. Reithler, M. Rieger, F. Scheuch, D. Teyssier, S. Thüer

RWTH Aachen University, III. Physikalisches Institut B, Aachen, GermanyG. Flügge, B. Kargoll, T. Kress, A. Künsken, J. Lingemann, T. Müller, A. Nehr Korn, A. Nowack, C. Pistone, O. Pooth, A. Stahl¹⁴**Deutsches Elektronen-Synchrotron, Hamburg, Germany**M. Aldaya Martin, T. Arndt, C. Asawatangtrakuldee, K. Beernaert, O. Behnke, U. Behrens, A. Bermúdez Martínez, A.A. Bin Anuar, K. Borras¹⁵, V. Botta, A. Campbell, P. Connor, C. Contreras-Campana, F. Costanza, C. Diez Pardos, G. Eckerlin, D. Eckstein, T. Eichhorn,

E. Eren, E. Gallo¹⁶, J. Garay Garcia, A. Geiser, A. Gizhko, J.M. Grados Luyando, A. Grohsjean, P. Gunnellini, M. Guthoff, A. Harb, J. Hauk, M. Hempel¹⁷, H. Jung, A. Kalogeropoulos, M. Kasemann, J. Keaveney, C. Kleinwort, I. Korol, D. Krücker, W. Lange, A. Lelek, T. Lenz, J. Leonard, K. Lipka, W. Lohmann¹⁷, R. Mankel, I.-A. Melzer-Pellmann, A.B. Meyer, G. Mittag, J. Mnich, A. Mussgiller, E. Ntomari, D. Pitzl, A. Raspereza, B. Roland, M. Savitskyi, P. Saxena, R. Shevchenko, S. Spannagel, N. Stefaniuk, G.P. Van Onsem, R. Walsh, Y. Wen, K. Wichmann, C. Wissing, O. Zenaiev

University of Hamburg, Hamburg, Germany

S. Bein, V. Blobel, M. Centis Vignali, T. Dreyer, E. Garutti, D. Gonzalez, J. Haller, A. Hinzmann, M. Hoffmann, A. Karavdina, R. Klanner, R. Kogler, N. Kovalchuk, S. Kurz, T. Lapsien, I. Marchesini, D. Marconi, M. Meyer, M. Niedziela, D. Nowatschin, F. Pantaleo¹⁴, T. Peiffer, A. Perieanu, C. Scharf, P. Schleper, A. Schmidt, S. Schumann, J. Schwandt, J. Sonneveld, H. Stadie, G. Steinbrück, F.M. Stober, M. Stöver, H. Tholen, D. Troendle, E. Usai, L. Vanelderen, A. Vanhoefer, B. Vormwald

Institut für Experimentelle Kernphysik, Karlsruhe, Germany

M. Akbiyik, C. Barth, S. Baur, E. Butz, R. Caspart, T. Chwalek, F. Colombo, W. De Boer, A. Dierlamm, B. Freund, R. Friese, M. Giffels, A. Gilbert, D. Haitz, F. Hartmann¹⁴, S.M. Heindl, U. Husemann, F. Kassel¹⁴, S. Kudella, H. Mildner, M.U. Mozer, Th. Müller, M. Plagge, G. Quast, K. Rabbertz, M. Schröder, I. Shvetsov, G. Sieber, H.J. Simonis, R. Ulrich, S. Wayand, M. Weber, T. Weiler, S. Williamson, C. Wöhrmann, R. Wolf

Institute of Nuclear and Particle Physics (INPP), NCSR Demokritos, Aghia Paraskevi, Greece

G. Anagnostou, G. Daskalakis, T. Gerasis, V.A. Giakoumopoulou, A. Kyriakis, D. Loukas, I. Topsis-Giotis

National and Kapodistrian University of Athens, Athens, Greece

G. Karathanasis, S. Kesisoglou, A. Panagiotou, N. Saoulidou

University of Ioánnina, Ioánnina, Greece

I. Evangelou, C. Foudas, P. Kokkas, S. Mallios, N. Manthos, I. Papadopoulos, E. Paradas, J. Strologas, F.A. Triantis

MTA-ELTE Lendület CMS Particle and Nuclear Physics Group, Eötvös Loránd University, Budapest, Hungary

M. Csanad, N. Filipovic, G. Pasztor, G.I. Veres¹⁸

Wigner Research Centre for Physics, Budapest, Hungary

G. Bencze, C. Hajdu, D. Horvath¹⁹, Á. Hunyadi, F. Sikler, V. Veszpremi, G. Vesztergombi¹⁸, A.J. Zsigmond

Institute of Nuclear Research ATOMKI, Debrecen, Hungary

N. Beni, S. Czellar, J. Karancsi²⁰, A. Makovec, J. Molnar, Z. Szillasi

Institute of Physics, University of Debrecen, Debrecen, Hungary

M. Bartók¹⁸, P. Raics, Z.L. Trocsanyi, B. Ujvari

Indian Institute of Science (IISc), Bangalore, India

S. Choudhury, J.R. Komaragiri

National Institute of Science Education and Research, Bhubaneswar, India

S. Bahinipati²¹, S. Bhowmik, P. Mal, K. Mandal, A. Nayak²², D.K. Sahoo²¹, N. Sahoo, S.K. Swain

Panjab University, Chandigarh, India

S. Bansal, S.B. Beri, V. Bhatnagar, R. Chawla, N. Dhingra, A.K. Kalsi, A. Kaur, M. Kaur, R. Kumar, P. Kumari, A. Mehta, J.B. Singh, G. Walia

University of Delhi, Delhi, India

Ashok Kumar, Aashaq Shah, A. Bhardwaj, S. Chauhan, B.C. Choudhary, R.B. Garg, S. Keshri, A. Kumar, S. Malhotra, M. Naimuddin, K. Ranjan, R. Sharma, V. Sharma

Saha Institute of Nuclear Physics, HBNI, Kolkata, India

R. Bhardwaj, R. Bhattacharya, S. Bhattacharya, U. Bhawandeep, S. Dey, S. Dutt, S. Dutta, S. Ghosh, N. Majumdar, A. Modak, K. Mondal, S. Mukhopadhyay, S. Nandan, A. Purohit, A. Roy, D. Roy, S. Roy Chowdhury, S. Sarkar, M. Sharan, S. Thakur

Indian Institute of Technology Madras, Madras, India

P.K. Behera

Bhabha Atomic Research Centre, Mumbai, India

R. Chudasama, D. Dutta, V. Jha, V. Kumar, A.K. Mohanty¹⁴, P.K. Netrakanti, L.M. Pant, P. Shukla, A. Topkar

Tata Institute of Fundamental Research-A, Mumbai, India

T. Aziz, S. Dugad, B. Mahakud, S. Mitra, G.B. Mohanty, N. Sur, B. Sutar

Tata Institute of Fundamental Research-B, Mumbai, India

S. Banerjee, S. Bhattacharya, S. Chatterjee, P. Das, M. Guchait, Sa. Jain, S. Kumar, M. Maity²³, G. Majumder, K. Mazumdar, T. Sarkar²³, N. Wickramage²⁴

Indian Institute of Science Education and Research (IISER), Pune, India

S. Chauhan, S. Dube, V. Hegde, A. Kapoor, K. Kothekar, S. Pandey, A. Rane, S. Sharma

Institute for Research in Fundamental Sciences (IPM), Tehran, Iran

S. Chenarani²⁵, E. Eskandari Tadavani, S.M. Etesami²⁵, M. Khakzad, M. Mohammadi Najafabadi, M. Naseri, S. Paktinat Mehdiabadi²⁶, F. Rezaei Hosseinabadi, B. Safarzadeh²⁷, M. Zeinali

University College Dublin, Dublin, Ireland

M. Felcini, M. Grunewald

INFN Sezione di Bari ^a, Università di Bari ^b, Politecnico di Bari ^c, Bari, Italy

M. Abbrescia^{a,b}, C. Calabria^{a,b}, C. Caputo^{a,b}, A. Colaleo^a, D. Creanza^{a,c}, L. Cristella^{a,b}, N. De Filippis^{a,c}, M. De Palma^{a,b}, F. Errico^{a,b}, L. Fiore^a, G. Iaselli^{a,c}, S. Lezki^{a,b}, G. Maggi^{a,c}, M. Maggi^a, G. Miniello^{a,b}, S. My^{a,b}, S. Nuzzo^{a,b}, A. Pompili^{a,b}, G. Pugliese^{a,c}, R. Radogna^{a,b}, A. Ranieri^a, G. Selvaggi^{a,b}, A. Sharma^a, L. Silvestris^{a,14}, R. Venditti^a, P. Verwilligen^a

INFN Sezione di Bologna ^a, Università di Bologna ^b, Bologna, Italy

G. Abbiendi^a, C. Battilana^{a,b}, D. Bonacorsi^{a,b}, S. Braibant-Giacomelli^{a,b}, R. Campanini^{a,b}, P. Capiluppi^{a,b}, A. Castro^{a,b}, F.R. Cavallo^a, S.S. Chhibra^a, G. Codispoti^{a,b}, M. Cuffiani^{a,b}, G.M. Dallavalle^a, F. Fabbri^a, A. Fanfani^{a,b}, D. Fasanella^{a,b}, P. Giacomelli^a, C. Grandi^a, L. Guiducci^{a,b}, S. Marcellini^a, G. Masetti^a, A. Montanari^a, F.L. Navarria^{a,b}, A. Perrotta^a, A.M. Rossi^{a,b}, T. Rovelli^{a,b}, G.P. Siroli^{a,b}, N. Tosi^a

INFN Sezione di Catania ^a, Università di Catania ^b, Catania, Italy

S. Albergo^{a,b}, S. Costa^{a,b}, A. Di Mattia^a, F. Giordano^{a,b}, R. Potenza^{a,b}, A. Tricomi^{a,b}, C. Tuve^{a,b}

INFN Sezione di Firenze ^a, Università di Firenze ^b, Firenze, Italy

G. Barbagli^a, K. Chatterjee^{a,b}, V. Ciulli^{a,b}, C. Civinini^a, R. D'Alessandro^{a,b}, E. Focardi^{a,b},
P. Lenzi^{a,b}, M. Meschini^a, S. Paoletti^a, L. Russo^{a,28}, G. Sguazzoni^a, D. Strom^a, L. Viliani^{a,b,14}

INFN Laboratori Nazionali di Frascati, Frascati, Italy

L. Benussi, S. Bianco, F. Fabbri, D. Piccolo, F. Primavera¹⁴

INFN Sezione di Genova ^a, Università di Genova ^b, Genova, Italy

V. Calvelli^{a,b}, F. Ferro^a, E. Robutti^a, S. Tosi^{a,b}

INFN Sezione di Milano-Bicocca ^a, Università di Milano-Bicocca ^b, Milano, Italy

L. Brianza^{a,b}, F. Brivio^{a,b}, V. Ciriolo^{a,b}, M.E. Dinardo^{a,b}, S. Fiorendi^{a,b}, S. Gennai^a, A. Ghezzi^{a,b},
P. Govoni^{a,b}, S. Gundacker, M. Malberti^{a,b}, S. Malvezzi^a, R.A. Manzoni^{a,b}, D. Menasce^a,
L. Moroni^a, M. Paganoni^{a,b}, K. Pauwels^{a,b}, D. Pedrini^a, S. Pigazzini^{a,b,29}, S. Ragazzi^{a,b},
T. Tabarelli de Fatis^{a,b}

INFN Sezione di Napoli ^a, Università di Napoli 'Federico II' ^b, Napoli, Italy, Università della Basilicata ^c, Potenza, Italy, Università G. Marconi ^d, Roma, Italy

S. Buontempo^a, N. Cavallo^{a,c}, S. Di Guida^{a,d,14}, F. Fabozzi^{a,c}, F. Fienga^{a,b}, A.O.M. Iorio^{a,b},
W.A. Khan^a, L. Lista^a, S. Meola^{a,d,14}, P. Paolucci^{a,14}, C. Sciacca^{a,b}, F. Thyssen^a

INFN Sezione di Padova ^a, Università di Padova ^b, Padova, Italy, Università di Trento ^c, Trento, Italy

P. Azzi^{a,14}, N. Bacchetta^a, L. Benato^{a,b}, D. Bisello^{a,b}, A. Boletti^{a,b}, R. Carlin^{a,b}, A. Carvalho
Antunes De Oliveira^{a,b}, P. Checchia^a, M. Dall'Osso^{a,b}, P. De Castro Manzano^a, T. Dorigo^a,
U. Dosselli^a, F. Gasparini^{a,b}, U. Gasparini^{a,b}, A. Gozzelino^a, S. Lacaprara^a, P. Lujan,
M. Margoni^{a,b}, A.T. Meneguzzo^{a,b}, N. Pozzobon^{a,b}, P. Ronchese^{a,b}, R. Rossin^{a,b}, F. Simonetto^{a,b},
E. Torassa^a, P. Zotto^{a,b}, G. Zumerle^{a,b}

INFN Sezione di Pavia ^a, Università di Pavia ^b, Pavia, Italy

A. Braghieri^a, A. Magnani^{a,b}, P. Montagna^{a,b}, S.P. Ratti^{a,b}, V. Re^a, M. Ressegotti, C. Riccardi^{a,b},
P. Salvini^a, I. Vai^{a,b}, P. Vitulo^{a,b}

INFN Sezione di Perugia ^a, Università di Perugia ^b, Perugia, Italy

L. Alunni Solestizi^{a,b}, M. Biasini^{a,b}, G.M. Bilei^a, C. Cecchi^{a,b}, D. Ciangottini^{a,b}, L. Fanò^{a,b},
P. Lariccia^{a,b}, R. Leonardi^{a,b}, E. Manoni^a, G. Mantovani^{a,b}, V. Mariani^{a,b}, M. Menichelli^a,
A. Rossi^{a,b}, A. Santocchia^{a,b}, D. Spiga^a

INFN Sezione di Pisa ^a, Università di Pisa ^b, Scuola Normale Superiore di Pisa ^c, Pisa, Italy

K. Androsov^a, P. Azzurri^{a,14}, G. Bagliesi^a, J. Bernardini^a, T. Boccali^a, L. Borrello, R. Castaldi^a,
M.A. Ciocci^{a,b}, R. Dell'Orso^a, G. Fedi^a, L. Giannini^{a,c}, A. Giassi^a, M.T. Grippo^{a,28}, F. Ligabue^{a,c},
T. Lomtadze^a, E. Manca^{a,c}, G. Mandorli^{a,c}, L. Martini^{a,b}, A. Messineo^{a,b}, F. Palla^a, A. Rizzi^{a,b},
A. Savoy-Navarro^{a,30}, P. Spagnolo^a, R. Tenchini^a, G. Tonelli^{a,b}, A. Venturi^a, P.G. Verdini^a

INFN Sezione di Roma ^a, Sapienza Università di Roma ^b, Rome, Italy

L. Barone^{a,b}, F. Cavallari^a, M. Cipriani^{a,b}, D. Del Re^{a,b,14}, E. Di Marco^{a,b,31}, M. Diemoz^a,
S. Gelli^{a,b}, E. Longo^{a,b}, F. Margaroli^{a,b}, B. Marzocchi^{a,b}, P. Meridiani^a, G. Organtini^{a,b},
R. Paramatti^{a,b}, F. Preiato^{a,b}, S. Rahatlou^{a,b}, C. Rovelli^a, F. Santanastasio^{a,b}

INFN Sezione di Torino ^a, Università di Torino ^b, Torino, Italy, Università del Piemonte Orientale ^c, Novara, Italy

N. Amapane^{a,b}, R. Arcidiacono^{a,c}, S. Argiro^{a,b}, M. Arneodo^{a,c}, N. Bartosik^a, R. Bellan^{a,b},
C. Biino^a, N. Cartiglia^a, F. Cenna^{a,b}, M. Costa^{a,b}, R. Covarelli^{a,b}, A. Degano^{a,b}, N. Demaria^a,
B. Kiani^{a,b}, C. Mariotti^a, S. Maselli^a, E. Migliore^{a,b}, V. Monaco^{a,b}, E. Monteil^{a,b}, M. Monteno^a,

M.M. Obertino^{a,b}, L. Pacher^{a,b}, N. Pastrone^a, M. Pelliccioni^a, G.L. Pinna Angioni^{a,b}, F. Ravera^{a,b}, A. Romero^{a,b}, M. Ruspa^{a,c}, R. Sacchi^{a,b}, K. Shchelina^{a,b}, V. Sola^a, A. Solano^{a,b}, A. Staiano^a, P. Traczyk^{a,b}

INFN Sezione di Trieste ^a, Università di Trieste ^b, Trieste, Italy

S. Belforte^a, M. Casarsa^a, F. Cossutti^a, G. Della Ricca^{a,b}, A. Zanetti^a

Kyungpook National University, Daegu, Korea

D.H. Kim, G.N. Kim, M.S. Kim, J. Lee, S. Lee, S.W. Lee, C.S. Moon, Y.D. Oh, S. Sekmen, D.C. Son, Y.C. Yang

Chonbuk National University, Jeonju, Korea

A. Lee

Chonnam National University, Institute for Universe and Elementary Particles, Kwangju, Korea

H. Kim, D.H. Moon, G. Oh

Hanyang University, Seoul, Korea

J.A. Brochero Cifuentes, J. Goh, T.J. Kim

Korea University, Seoul, Korea

S. Cho, S. Choi, Y. Go, D. Gyun, S. Ha, B. Hong, Y. Jo, Y. Kim, K. Lee, K.S. Lee, S. Lee, J. Lim, S.K. Park, Y. Roh

Seoul National University, Seoul, Korea

J. Almond, J. Kim, J.S. Kim, H. Lee, K. Lee, K. Nam, S.B. Oh, B.C. Radburn-Smith, S.h. Seo, U.K. Yang, H.D. Yoo, G.B. Yu

University of Seoul, Seoul, Korea

M. Choi, H. Kim, J.H. Kim, J.S.H. Lee, I.C. Park

Sungkyunkwan University, Suwon, Korea

Y. Choi, C. Hwang, J. Lee, I. Yu

Vilnius University, Vilnius, Lithuania

V. Dudenas, A. Juodagalvis, J. Vaitkus

National Centre for Particle Physics, Universiti Malaya, Kuala Lumpur, Malaysia

I. Ahmed, Z.A. Ibrahim, M.A.B. Md Ali³², F. Mohamad Idris³³, W.A.T. Wan Abdullah, M.N. Yusli, Z. Zolkapli

Centro de Investigacion y de Estudios Avanzados del IPN, Mexico City, Mexico

Reyes-Almanza, R, Ramirez-Sanchez, G., Duran-Osuna, M. C., H. Castilla-Valdez, E. De La Cruz-Burelo, I. Heredia-De La Cruz³⁴, Rabadan-Trejo, R. I., R. Lopez-Fernandez, J. Mejia Guisao, A. Sanchez-Hernandez

Universidad Iberoamericana, Mexico City, Mexico

S. Carrillo Moreno, C. Oropeza Barrera, F. Vazquez Valencia

Benemerita Universidad Autonoma de Puebla, Puebla, Mexico

I. Pedraza, H.A. Salazar Ibarguen, C. Uribe Estrada

Universidad Autónoma de San Luis Potosí, San Luis Potosí, Mexico

A. Morelos Pineda

University of Auckland, Auckland, New Zealand

D. Krofcheck

University of Canterbury, Christchurch, New Zealand

P.H. Butler

National Centre for Physics, Quaid-I-Azam University, Islamabad, Pakistan

A. Ahmad, M. Ahmad, Q. Hassan, H.R. Hoorani, A. Saddique, M.A. Shah, M. Shoaib, M. Waqas

National Centre for Nuclear Research, Swierk, Poland

H. Bialkowska, M. Bluj, B. Boimska, T. Frueboes, M. Górski, M. Kazana, K. Nawrocki, M. Szleper, P. Zalewski

Institute of Experimental Physics, Faculty of Physics, University of Warsaw, Warsaw, PolandK. Bunkowski, A. Byszuk³⁵, K. Doroba, A. Kalinowski, M. Konecki, J. Krolikowski, M. Misiura, M. Olszewski, A. Pyskir, M. Walczak**Laboratório de Instrumentação e Física Experimental de Partículas, Lisboa, Portugal**

P. Bargassa, C. Beirão Da Cruz E Silva, A. Di Francesco, P. Faccioli, M. Gallinaro, J. Hollar, N. Leonardo, L. Lloret Iglesias, M.V. Nemallapudi, J. Seixas, O. Toldaiev, D. Vadrucchio, J. Varela

Joint Institute for Nuclear Research, Dubna, RussiaS. Afanasiev, P. Bunin, M. Gavrilenko, I. Golutvin, I. Gorbunov, A. Kamenev, V. Karjavin, A. Lanev, A. Malakhov, V. Matveev^{36,37}, V. Palichik, V. Perelygin, S. Shmatov, S. Shulha, N. Skatchkov, V. Smirnov, N. Voytishin, A. Zarubin**Petersburg Nuclear Physics Institute, Gatchina (St. Petersburg), Russia**Y. Ivanov, V. Kim³⁸, E. Kuznetsova³⁹, P. Levchenko, V. Murzin, V. Oreshkin, I. Smirnov, V. Sulimov, L. Uvarov, S. Vavilov, A. Vorobyev**Institute for Nuclear Research, Moscow, Russia**

Yu. Andreev, A. Dermenev, S. Gninenko, N. Golubev, A. Karneyeu, M. Kirsanov, N. Krasnikov, A. Pashenkov, D. Tlisov, A. Toropin

Institute for Theoretical and Experimental Physics, Moscow, Russia

V. Epshteyn, V. Gavrilov, N. Lychkovskaya, V. Popov, I. Pozdnyakov, G. Safronov, A. Spiridonov, A. Stepenov, M. Toms, E. Vlasov, A. Zhokin

Moscow Institute of Physics and Technology, Moscow, RussiaT. Aushev, A. Bylinkin³⁷**National Research Nuclear University 'Moscow Engineering Physics Institute' (MEPhI), Moscow, Russia**R. Chistov⁴⁰, M. Danilov⁴⁰, P. Parygin, D. Philippov, S. Polikarpov, E. Tarkovskii**P.N. Lebedev Physical Institute, Moscow, Russia**V. Andreev, M. Azarkin³⁷, I. Dremin³⁷, M. Kirakosyan³⁷, A. Terkulov**Skobeltsyn Institute of Nuclear Physics, Lomonosov Moscow State University, Moscow, Russia**A. Baskakov, A. Belyaev, E. Boos, V. Bunichev, M. Dubinin⁴¹, L. Dudko, A. Gribushin, V. Klyukhin, O. Kodolova, I. Lokhtin, I. Miagkov, S. Obraztsov, S. Petrushanko, V. Savrin, A. Snigirev**Novosibirsk State University (NSU), Novosibirsk, Russia**V. Blinov⁴², Y. Skovpen⁴², D. Shtol⁴²

State Research Center of Russian Federation, Institute for High Energy Physics, Protvino, Russia

I. Azhgirey, I. Bayshev, S. Bitioukov, D. Elumakhov, V. Kachanov, A. Kalinin, D. Konstantinov, V. Krychkin, V. Petrov, R. Ryutin, A. Sobol, S. Troshin, N. Tyurin, A. Uzunian, A. Volkov

University of Belgrade, Faculty of Physics and Vinca Institute of Nuclear Sciences, Belgrade, Serbia

P. Adzic⁴³, P. Cirkovic, D. Devetak, M. Dordevic, J. Milosevic, V. Rekovic

Centro de Investigaciones Energéticas Medioambientales y Tecnológicas (CIEMAT), Madrid, Spain

J. Alcaraz Maestre, M. Barrio Luna, M. Cerrada, N. Colino, B. De La Cruz, A. Delgado Peris, A. Escalante Del Valle, C. Fernandez Bedoya, J.P. Fernández Ramos, J. Flix, M.C. Fouz, P. Garcia-Abia, O. Gonzalez Lopez, S. Goy Lopez, J.M. Hernandez, M.I. Josa, A. Pérez-Calero Yzquierdo, J. Puerta Pelayo, A. Quintario Olmeda, I. Redondo, L. Romero, M.S. Soares, A. Álvarez Fernández

Universidad Autónoma de Madrid, Madrid, Spain

J.F. de Trocóniz, M. Missiroli, D. Moran

Universidad de Oviedo, Oviedo, Spain

J. Cuevas, C. Erice, J. Fernandez Menendez, I. Gonzalez Caballero, J.R. González Fernández, E. Palencia Cortezon, S. Sanchez Cruz, I. Suárez Andrés, P. Vischia, J.M. Vizán García

Instituto de Física de Cantabria (IFCA), CSIC-Universidad de Cantabria, Santander, Spain

I.J. Cabrillo, A. Calderon, B. Chazin Quero, E. Curras, J. Duarte Campderros, M. Fernandez, J. Garcia-Ferrero, G. Gomez, A. Lopez Virto, J. Marco, C. Martinez Rivero, P. Martinez Ruiz del Arbol, F. Matorras, J. Piedra Gomez, T. Rodrigo, A. Ruiz-Jimeno, L. Scodellaro, N. Trevisani, I. Vila, R. Vilar Cortabitarte

CERN, European Organization for Nuclear Research, Geneva, Switzerland

D. Abbaneo, E. Auffray, P. Baillon, A.H. Ball, D. Barney, M. Bianco, P. Bloch, A. Bocci, C. Botta, T. Camporesi, R. Castello, M. Cepeda, G. Cerminara, E. Chapon, Y. Chen, D. d'Enterria, A. Dabrowski, V. Daponte, A. David, M. De Gruttola, A. De Roeck, M. Dobson, B. Dorney, T. du Pree, M. Dünser, N. Dupont, A. Elliott-Peisert, P. Everaerts, F. Fallavollita, G. Franzoni, J. Fulcher, W. Funk, D. Gigi, K. Gill, F. Glege, D. Gulhan, P. Harris, J. Hegeman, V. Innocente, P. Janot, O. Karacheban¹⁷, J. Kieseler, H. Kirschenmann, V. Knünz, A. Kornmayer¹⁴, M.J. Kortelainen, M. Krammer¹, C. Lange, P. Lecoq, C. Lourenço, M.T. Lucchini, L. Malgeri, M. Mannelli, A. Martelli, F. Meijers, J.A. Merlin, S. Mersi, E. Meschi, P. Milenovic⁴⁴, F. Moortgat, M. Mulders, H. Neugebauer, S. Orfanelli, L. Orsini, L. Pape, E. Perez, M. Peruzzi, A. Petrilli, G. Petrucciani, A. Pfeiffer, M. Pierini, A. Racz, T. Reis, G. Rolandi⁴⁵, M. Rovere, H. Sakulin, C. Schäfer, C. Schwick, M. Seidel, M. Selvaggi, A. Sharma, P. Silva, P. Sphicas⁴⁶, A. Stakia, J. Steggemann, M. Stoye, M. Tosi, D. Treille, A. Triossi, A. Tsiros, V. Veckalns⁴⁷, M. Verweij, W.D. Zeuner

Paul Scherrer Institut, Villigen, Switzerland

W. Bertl[†], L. Caminada⁴⁸, K. Deiters, W. Erdmann, R. Horisberger, Q. Ingram, H.C. Kaestli, D. Kotlinski, U. Langenegger, T. Rohe, S.A. Wiederkehr

Institute for Particle Physics, ETH Zurich, Zurich, Switzerland

F. Bachmair, L. Bäni, P. Berger, L. Bianchini, B. Casal, G. Dissertori, M. Dittmar, M. Donegà, C. Grab, C. Heidegger, D. Hits, J. Hoss, G. Kasieczka, T. Klijnsma, W. Lustermann, B. Mangano, M. Marionneau, M.T. Meinhard, D. Meister, F. Micheli, P. Musella, F. Nessi-Tedaldi, F. Pandolfi,

J. Pata, F. Pauss, G. Perrin, L. Perrozzi, M. Quittnat, M. Reichmann, M. Schönenberger, L. Shchutska, V.R. Tavolaro, K. Theofilatos, M.L. Vesterbacka Olsson, R. Wallny, D.H. Zhu

Universität Zürich, Zurich, Switzerland

T.K. Aarrestad, C. Amsler⁴⁹, M.F. Canelli, A. De Cosa, R. Del Burgo, S. Donato, C. Galloni, T. Hreus, B. Kilminster, J. Ngadiuba, D. Pinna, G. Rauco, P. Robmann, D. Salerno, C. Seitz, Y. Takahashi, A. Zucchetta

National Central University, Chung-Li, Taiwan

V. Candelise, T.H. Doan, Sh. Jain, R. Khurana, C.M. Kuo, W. Lin, A. Pozdnyakov, S.S. Yu

National Taiwan University (NTU), Taipei, Taiwan

Arun Kumar, P. Chang, Y. Chao, K.F. Chen, P.H. Chen, F. Fiori, W.-S. Hou, Y. Hsiung, Y.F. Liu, R.-S. Lu, E. Paganis, A. Psallidas, A. Steen, J.f. Tsai

Chulalongkorn University, Faculty of Science, Department of Physics, Bangkok, Thailand

B. Asavapibhop, K. Kovitanggoon, G. Singh, N. Srimanobhas

Çukurova University, Physics Department, Science and Art Faculty, Adana, Turkey

A. Adiguzel⁵⁰, F. Boran, S. Cerci⁵¹, S. Damarseckin, Z.S. Demiroglu, C. Dozen, I. Dumanoglu, S. Girgis, G. Gokbulut, Y. Guler, I. Hos⁵², E.E. Kangal⁵³, O. Kara, A. Kayis Topaksu, U. Kiminsu, M. Oglakci, G. Onengut⁵⁴, K. Ozdemir⁵⁵, D. Sunar Cerci⁵¹, B. Tali⁵¹, S. Turkcapar, I.S. Zorbakir, C. Zorbilmez

Middle East Technical University, Physics Department, Ankara, Turkey

B. Bilin, G. Karapinar⁵⁶, K. Ocalan⁵⁷, M. Yalvac, M. Zeyrek

Bogazici University, Istanbul, Turkey

E. Gülmez, M. Kaya⁵⁸, O. Kaya⁵⁹, S. Tekten, E.A. Yetkin⁶⁰

Istanbul Technical University, Istanbul, Turkey

M.N. Agaras, S. Atay, A. Cakir, K. Cankocak

Institute for Scintillation Materials of National Academy of Science of Ukraine, Kharkov, Ukraine

B. Grynyov

National Scientific Center, Kharkov Institute of Physics and Technology, Kharkov, Ukraine

L. Levchuk, P. Sorokin

University of Bristol, Bristol, United Kingdom

R. Aggleton, F. Ball, L. Beck, J.J. Brooke, D. Burns, E. Clement, D. Cussans, O. Davignon, H. Flacher, J. Goldstein, M. Grimes, G.P. Heath, H.F. Heath, J. Jacob, L. Kreczko, C. Lucas, D.M. Newbold⁶¹, S. Paramesvaran, A. Poll, T. Sakuma, S. Seif El Nasr-storey, D. Smith, V.J. Smith

Rutherford Appleton Laboratory, Didcot, United Kingdom

K.W. Bell, A. Belyaev⁶², C. Brew, R.M. Brown, L. Calligaris, D. Cieri, D.J.A. Cockerill, J.A. Coughlan, K. Harder, S. Harper, E. Olaiya, D. Petyt, C.H. Shepherd-Themistocleous, A. Thea, I.R. Tomalin, T. Williams

Imperial College, London, United Kingdom

G. Auzinger, R. Bainbridge, S. Breeze, O. Buchmuller, A. Bundock, S. Casasso, M. Citron, D. Colling, L. Corpe, P. Dauncey, G. Davies, A. De Wit, M. Della Negra, R. Di Maria, A. Elwood, Y. Haddad, G. Hall, G. Iles, T. James, R. Lane, C. Laner, L. Lyons, A.-M. Magnan, S. Malik, L. Mastrolorenzo, T. Matsushita, J. Nash, A. Nikitenko⁶, V. Palladino, M. Pesaresi,

D.M. Raymond, A. Richards, A. Rose, E. Scott, C. Seez, A. Shtipliyski, S. Summers, A. Tapper, K. Uchida, M. Vazquez Acosta⁶³, T. Virdee¹⁴, N. Wardle, D. Winterbottom, J. Wright, S.C. Zenz

Brunel University, Uxbridge, United Kingdom

J.E. Cole, P.R. Hobson, A. Khan, P. Kyberd, I.D. Reid, P. Symonds, L. Teodorescu, M. Turner

Baylor University, Waco, USA

A. Borzou, K. Call, J. Dittmann, K. Hatakeyama, H. Liu, N. Pastika, C. Smith

Catholic University of America, Washington DC, USA

R. Bartek, A. Dominguez

The University of Alabama, Tuscaloosa, USA

A. Buccilli, S.I. Cooper, C. Henderson, P. Rumerio, C. West

Boston University, Boston, USA

D. Arcaro, A. Avetisyan, T. Bose, D. Gastler, D. Rankin, C. Richardson, J. Rohlf, L. Sulak, D. Zou

Brown University, Providence, USA

G. Benelli, D. Cutts, A. Garabedian, J. Hakala, U. Heintz, J.M. Hogan, K.H.M. Kwok, E. Laird, G. Landsberg, Z. Mao, M. Narain, J. Pazzini, S. Piperov, S. Sagir, R. Syarif, D. Yu

University of California, Davis, Davis, USA

R. Band, C. Brainerd, D. Burns, M. Calderon De La Barca Sanchez, M. Chertok, J. Conway, R. Conway, P.T. Cox, R. Erbacher, C. Flores, G. Funk, M. Gardner, W. Ko, R. Lander, C. Mclean, M. Mulhearn, D. Pellett, J. Pilot, S. Shalhout, M. Shi, J. Smith, M. Squires, D. Stolp, K. Tos, M. Tripathi, Z. Wang

University of California, Los Angeles, USA

M. Bachtis, C. Bravo, R. Cousins, A. Dasgupta, A. Florent, J. Hauser, M. Ignatenko, N. Mccoll, D. Saltzberg, C. Schnaible, V. Valuev

University of California, Riverside, Riverside, USA

E. Bouvier, K. Burt, R. Clare, J. Ellison, J.W. Gary, S.M.A. Ghiasi Shirazi, G. Hanson, J. Heilman, P. Jandir, E. Kennedy, F. Lacroix, O.R. Long, M. Olmedo Negrete, M.I. Paneva, A. Shrinivas, W. Si, L. Wang, H. Wei, S. Wimpenny, B. R. Yates

University of California, San Diego, La Jolla, USA

J.G. Branson, S. Cittolin, M. Derdzinski, B. Hashemi, A. Holzner, D. Klein, G. Kole, V. Krutelyov, J. Letts, I. Macneill, M. Masciovecchio, D. Olivito, S. Padhi, M. Pieri, M. Sani, V. Sharma, S. Simon, M. Tadel, A. Vartak, S. Wasserbaech⁶⁴, J. Wood, F. Würthwein, A. Yagil, G. Zevi Della Porta

University of California, Santa Barbara - Department of Physics, Santa Barbara, USA

N. Amin, R. Bhandari, J. Bradmiller-Feld, C. Campagnari, A. Dishaw, V. Dutta, M. Franco Sevilla, C. George, F. Golf, L. Gouskos, J. Gran, R. Heller, J. Incandela, S.D. Mullin, A. Ovcharova, H. Qu, J. Richman, D. Stuart, I. Suarez, J. Yoo

California Institute of Technology, Pasadena, USA

D. Anderson, J. Bendavid, A. Bornheim, J.M. Lawhorn, H.B. Newman, T. Nguyen, C. Pena, M. Spiropulu, J.R. Vlimant, S. Xie, Z. Zhang, R.Y. Zhu

Carnegie Mellon University, Pittsburgh, USA

M.B. Andrews, T. Ferguson, T. Mudholkar, M. Paulini, J. Russ, M. Sun, H. Vogel, I. Vorobiev, M. Weinberg

University of Colorado Boulder, Boulder, USA

J.P. Cumalat, W.T. Ford, F. Jensen, A. Johnson, M. Krohn, S. Leontsinis, T. Mulholland, K. Stenson, S.R. Wagner

Cornell University, Ithaca, USA

J. Alexander, J. Chaves, J. Chu, S. Dittmer, K. McDermott, N. Mirman, J.R. Patterson, A. Rinkevicius, A. Ryd, L. Skinnari, L. Soffi, S.M. Tan, Z. Tao, J. Thom, J. Tucker, P. Wittich, M. Zientek

Fermi National Accelerator Laboratory, Batavia, USA

S. Abdullin, M. Albrow, G. Apollinari, A. Apresyan, A. Apyan, S. Banerjee, L.A.T. Bauerdick, A. Beretvas, J. Berryhill, P.C. Bhat, G. Bolla, K. Burkett, J.N. Butler, A. Canepa, G.B. Cerati, H.W.K. Cheung, F. Chlebana, M. Cremonesi, J. Duarte, V.D. Elvira, J. Freeman, Z. Gecse, E. Gottschalk, L. Gray, D. Green, S. Grünendahl, O. Gutsche, R.M. Harris, S. Hasegawa, J. Hirschauer, Z. Hu, B. Jayatilaka, S. Jindariani, M. Johnson, U. Joshi, B. Klima, B. Kreis, S. Lammel, D. Lincoln, R. Lipton, M. Liu, T. Liu, R. Lopes De Sá, J. Lykken, K. Maeshima, N. Magini, J.M. Marraffino, S. Maruyama, D. Mason, P. McBride, P. Merkel, S. Mrenna, S. Nahn, V. O'Dell, K. Pedro, O. Prokofyev, G. Rakness, L. Ristori, B. Schneider, E. Sexton-Kennedy, A. Soha, W.J. Spalding, L. Spiegel, S. Stoynev, J. Strait, N. Strobbe, L. Taylor, S. Tkaczyk, N.V. Tran, L. Uplegger, E.W. Vaandering, C. Vernieri, M. Verzocchi, R. Vidal, M. Wang, H.A. Weber, A. Whitbeck

University of Florida, Gainesville, USA

D. Acosta, P. Avery, P. Bortignon, D. Bourilkov, A. Brinkerhoff, A. Carnes, M. Carver, D. Curry, R.D. Field, I.K. Furic, J. Konigsberg, A. Korytov, K. Kotov, P. Ma, K. Matchev, H. Mei, G. Mitselmakher, D. Rank, D. Sperka, N. Terentyev, L. Thomas, J. Wang, S. Wang, J. Yelton

Florida International University, Miami, USA

Y.R. Joshi, S. Linn, P. Markowitz, J.L. Rodriguez

Florida State University, Tallahassee, USA

A. Ackert, T. Adams, A. Askew, S. Hagopian, V. Hagopian, K.F. Johnson, T. Kolberg, G. Martinez, T. Perry, H. Prosper, A. Saha, A. Santra, R. Yohay

Florida Institute of Technology, Melbourne, USA

M.M. Baarmand, V. Bhopatkar, S. Colafranceschi, M. Hohlmann, D. Noonan, T. Roy, F. Yumiceva

University of Illinois at Chicago (UIC), Chicago, USA

M.R. Adams, L. Apanasevich, D. Berry, R.R. Betts, R. Cavanaugh, X. Chen, O. Evdokimov, C.E. Gerber, D.A. Hangal, D.J. Hofman, K. Jung, J. Kamin, I.D. Sandoval Gonzalez, M.B. Tonjes, H. Trauger, N. Varelas, H. Wang, Z. Wu, J. Zhang

The University of Iowa, Iowa City, USA

B. Bilki⁶⁵, W. Clarida, K. Dilsiz⁶⁶, S. Durgut, R.P. Gandrajula, M. Haytmyradov, V. Khristenko, J.-P. Merlo, H. Mermerkaya⁶⁷, A. Mestvirishvili, A. Moeller, J. Nachtman, H. Ogul⁶⁸, Y. Onel, F. Ozok⁶⁹, A. Penzo, C. Snyder, E. Tiras, J. Wetzel, K. Yi

Johns Hopkins University, Baltimore, USA

B. Blumenfeld, A. Cocoros, N. Eminizer, D. Fehling, L. Feng, A.V. Gritsan, P. Maksimovic, J. Roskes, U. Sarica, M. Swartz, M. Xiao, C. You

The University of Kansas, Lawrence, USA

A. Al-bataineh, P. Baringer, A. Bean, S. Boren, J. Bowen, J. Castle, S. Khalil, A. Kropivnitskaya,

D. Majumder, W. Mcbrayer, M. Murray, C. Royon, S. Sanders, E. Schmitz, R. Stringer, J.D. Tapia Takaki, Q. Wang

Kansas State University, Manhattan, USA

A. Ivanov, K. Kaadze, Y. Maravin, A. Mohammadi, L.K. Saini, N. Skhirtladze, S. Toda

Lawrence Livermore National Laboratory, Livermore, USA

F. Rebassoo, D. Wright

University of Maryland, College Park, USA

C. Anelli, A. Baden, O. Baron, A. Belloni, B. Calvert, S.C. Eno, C. Ferraioli, N.J. Hadley, S. Jabeen, G.Y. Jeng, R.G. Kellogg, J. Kunkle, A.C. Mignerey, F. Ricci-Tam, Y.H. Shin, A. Skuja, S.C. Tonwar

Massachusetts Institute of Technology, Cambridge, USA

D. Abercrombie, B. Allen, V. Azzolini, R. Barbieri, A. Baty, R. Bi, S. Brandt, W. Busza, I.A. Cali, M. D'Alfonso, Z. Demiragli, G. Gomez Ceballos, M. Goncharov, D. Hsu, Y. Iiyama, G.M. Innocenti, M. Klute, D. Kovalskyi, Y.S. Lai, Y.-J. Lee, A. Levin, P.D. Luckey, B. Maier, A.C. Marini, C. McGinn, C. Mironov, S. Narayanan, X. Niu, C. Paus, C. Roland, G. Roland, J. Salfeld-Nebgen, G.S.F. Stephans, K. Tatar, D. Velicanu, J. Wang, T.W. Wang, B. Wyslouch

University of Minnesota, Minneapolis, USA

A.C. Benvenuti, R.M. Chatterjee, A. Evans, P. Hansen, S. Kalafut, Y. Kubota, Z. Lesko, J. Mans, S. Nourbakhsh, N. Ruckstuhl, R. Rusack, J. Turkewitz

University of Mississippi, Oxford, USA

J.G. Acosta, S. Oliveros

University of Nebraska-Lincoln, Lincoln, USA

E. Avdeeva, K. Bloom, D.R. Claes, C. Fangmeier, R. Gonzalez Suarez, R. Kamalieddin, I. Kravchenko, J. Monroy, J.E. Siado, G.R. Snow, B. Stieger

State University of New York at Buffalo, Buffalo, USA

M. Alyari, J. Dolen, A. Godshalk, C. Harrington, I. Iashvili, D. Nguyen, A. Parker, S. Rappoccio, B. Roozbahani

Northeastern University, Boston, USA

G. Alverson, E. Barberis, A. Hortiangtham, A. Massironi, D.M. Morse, D. Nash, T. Orimoto, R. Teixeira De Lima, D. Trocino, D. Wood

Northwestern University, Evanston, USA

S. Bhattacharya, O. Charaf, K.A. Hahn, N. Mucia, N. Odell, B. Pollack, M.H. Schmitt, K. Sung, M. Trovato, M. Velasco

University of Notre Dame, Notre Dame, USA

N. Dev, M. Hildreth, K. Hurtado Anampa, C. Jessop, D.J. Karmgard, N. Kellams, K. Lannon, N. Loukas, N. Marinelli, F. Meng, C. Mueller, Y. Musienko³⁶, M. Planer, A. Reinsvold, R. Ruchti, G. Smith, S. Taroni, M. Wayne, M. Wolf, A. Woodard

The Ohio State University, Columbus, USA

J. Alimena, L. Antonelli, B. Bylsma, L.S. Durkin, S. Flowers, B. Francis, A. Hart, C. Hill, W. Ji, B. Liu, W. Luo, D. Puigh, B.L. Winer, H.W. Wulsin

Princeton University, Princeton, USA

A. Benaglia, S. Cooperstein, O. Driga, P. Elmer, J. Hardenbrook, P. Hebda, S. Higginbotham,

D. Lange, J. Luo, D. Marlow, K. Mei, I. Ojalvo, J. Olsen, C. Palmer, P. Piroué, D. Stickland, C. Tully

University of Puerto Rico, Mayaguez, USA

S. Malik, S. Norberg

Purdue University, West Lafayette, USA

A. Barker, V.E. Barnes, S. Das, S. Folgueras, L. Gutay, M.K. Jha, M. Jones, A.W. Jung, A. Khatiwada, D.H. Miller, N. Neumeister, C.C. Peng, J.F. Schulte, J. Sun, F. Wang, W. Xie

Purdue University Northwest, Hammond, USA

T. Cheng, N. Parashar, J. Stupak

Rice University, Houston, USA

A. Adair, B. Akgun, Z. Chen, K.M. Ecklund, F.J.M. Geurts, M. Guilbaud, W. Li, B. Michlin, M. Northup, B.P. Padley, J. Roberts, J. Rorie, Z. Tu, J. Zabel

University of Rochester, Rochester, USA

A. Bodek, P. de Barbaro, R. Demina, Y.t. Duh, T. Ferbel, M. Galanti, A. Garcia-Bellido, J. Han, O. Hindrichs, A. Khukhunaishvili, K.H. Lo, P. Tan, M. Verzetti

The Rockefeller University, New York, USA

R. Ciesielski, K. Goulianos, C. Mesropian

Rutgers, The State University of New Jersey, Piscataway, USA

A. Agapitos, J.P. Chou, Y. Gershtein, T.A. Gómez Espinosa, E. Halkiadakis, M. Heindl, E. Hughes, S. Kaplan, R. Kunnawalkam Elayavalli, S. Kyriacou, A. Lath, R. Montalvo, K. Nash, M. Osherson, H. Saka, S. Salur, S. Schnetzer, D. Sheffield, S. Somalwar, R. Stone, S. Thomas, P. Thomassen, M. Walker

University of Tennessee, Knoxville, USA

A.G. Delannoy, M. Foerster, J. Heideman, G. Riley, K. Rose, S. Spanier, K. Thapa

Texas A&M University, College Station, USA

O. Bouhali⁷⁰, A. Castaneda Hernandez⁷⁰, A. Celik, M. Dalchenko, M. De Mattia, A. Delgado, S. Dildick, R. Eusebi, J. Gilmore, T. Huang, T. Kamon⁷¹, R. Mueller, Y. Pakhotin, R. Patel, A. Perloff, L. Perniè, D. Rathjens, A. Safonov, A. Tatarinov, K.A. Ulmer

Texas Tech University, Lubbock, USA

N. Akchurin, J. Damgov, F. De Guio, P.R. Duderod, J. Faulkner, E. Gurpinar, S. Kunori, K. Lamichhane, S.W. Lee, T. Libeiro, T. Peltola, S. Undleeb, I. Volobouev, Z. Wang

Vanderbilt University, Nashville, USA

S. Greene, A. Gurrola, R. Janjam, W. Johns, C. Maguire, A. Melo, H. Ni, P. Sheldon, S. Tuo, J. Velkovska, Q. Xu

University of Virginia, Charlottesville, USA

M.W. Arenton, P. Barria, B. Cox, R. Hirosky, A. Ledovskoy, H. Li, C. Neu, T. Sinthuprasith, X. Sun, Y. Wang, E. Wolfe, F. Xia

Wayne State University, Detroit, USA

R. Harr, P.E. Karchin, J. Sturdy, S. Zaleski

University of Wisconsin - Madison, Madison, WI, USA

M. Brodski, J. Buchanan, C. Caillol, S. Dasu, L. Dodd, S. Duric, B. Gomber, M. Grothe,

M. Herndon, A. Hervé, U. Hussain, P. Klabbers, A. Lanaro, A. Levine, K. Long, R. Loveless, G.A. Pierro, G. Polese, T. Ruggles, A. Savin, N. Smith, W.H. Smith, D. Taylor, N. Woods

†: Deceased

- 1: Also at Vienna University of Technology, Vienna, Austria
- 2: Also at State Key Laboratory of Nuclear Physics and Technology, Peking University, Beijing, China
- 3: Also at Universidade Estadual de Campinas, Campinas, Brazil
- 4: Also at Universidade Federal de Pelotas, Pelotas, Brazil
- 5: Also at Université Libre de Bruxelles, Bruxelles, Belgium
- 6: Also at Institute for Theoretical and Experimental Physics, Moscow, Russia
- 7: Also at Joint Institute for Nuclear Research, Dubna, Russia
- 8: Also at Suez University, Suez, Egypt
- 9: Now at British University in Egypt, Cairo, Egypt
- 10: Now at Helwan University, Cairo, Egypt
- 11: Also at Université de Haute Alsace, Mulhouse, France
- 12: Also at Skobeltsyn Institute of Nuclear Physics, Lomonosov Moscow State University, Moscow, Russia
- 13: Also at Tbilisi State University, Tbilisi, Georgia
- 14: Also at CERN, European Organization for Nuclear Research, Geneva, Switzerland
- 15: Also at RWTH Aachen University, III. Physikalisches Institut A, Aachen, Germany
- 16: Also at University of Hamburg, Hamburg, Germany
- 17: Also at Brandenburg University of Technology, Cottbus, Germany
- 18: Also at MTA-ELTE Lendület CMS Particle and Nuclear Physics Group, Eötvös Loránd University, Budapest, Hungary
- 19: Also at Institute of Nuclear Research ATOMKI, Debrecen, Hungary
- 20: Also at Institute of Physics, University of Debrecen, Debrecen, Hungary
- 21: Also at Indian Institute of Technology Bhubaneswar, Bhubaneswar, India
- 22: Also at Institute of Physics, Bhubaneswar, India
- 23: Also at University of Visva-Bharati, Santiniketan, India
- 24: Also at University of Ruhuna, Matara, Sri Lanka
- 25: Also at Isfahan University of Technology, Isfahan, Iran
- 26: Also at Yazd University, Yazd, Iran
- 27: Also at Plasma Physics Research Center, Science and Research Branch, Islamic Azad University, Tehran, Iran
- 28: Also at Università degli Studi di Siena, Siena, Italy
- 29: Also at INFN Sezione di Milano-Bicocca; Università di Milano-Bicocca, Milano, Italy
- 30: Also at Purdue University, West Lafayette, USA
- 31: Also at INFN Sezione di Roma; Sapienza Università di Roma, Rome, Italy
- 32: Also at International Islamic University of Malaysia, Kuala Lumpur, Malaysia
- 33: Also at Malaysian Nuclear Agency, MOSTI, Kajang, Malaysia
- 34: Also at Consejo Nacional de Ciencia y Tecnología, Mexico city, Mexico
- 35: Also at Warsaw University of Technology, Institute of Electronic Systems, Warsaw, Poland
- 36: Also at Institute for Nuclear Research, Moscow, Russia
- 37: Now at National Research Nuclear University 'Moscow Engineering Physics Institute' (MEPhI), Moscow, Russia
- 38: Also at St. Petersburg State Polytechnical University, St. Petersburg, Russia
- 39: Also at University of Florida, Gainesville, USA
- 40: Also at P.N. Lebedev Physical Institute, Moscow, Russia
- 41: Also at California Institute of Technology, Pasadena, USA

- 42: Also at Budker Institute of Nuclear Physics, Novosibirsk, Russia
- 43: Also at Faculty of Physics, University of Belgrade, Belgrade, Serbia
- 44: Also at University of Belgrade, Faculty of Physics and Vinca Institute of Nuclear Sciences, Belgrade, Serbia
- 45: Also at Scuola Normale e Sezione dell'INFN, Pisa, Italy
- 46: Also at National and Kapodistrian University of Athens, Athens, Greece
- 47: Also at Riga Technical University, Riga, Latvia
- 48: Also at Universität Zürich, Zurich, Switzerland
- 49: Also at Stefan Meyer Institute for Subatomic Physics (SMI), Vienna, Austria
- 50: Also at Istanbul University, Faculty of Science, Istanbul, Turkey
- 51: Also at Adiyaman University, Adiyaman, Turkey
- 52: Also at Istanbul Aydin University, Istanbul, Turkey
- 53: Also at Mersin University, Mersin, Turkey
- 54: Also at Cag University, Mersin, Turkey
- 55: Also at Piri Reis University, Istanbul, Turkey
- 56: Also at Izmir Institute of Technology, Izmir, Turkey
- 57: Also at Necmettin Erbakan University, Konya, Turkey
- 58: Also at Marmara University, Istanbul, Turkey
- 59: Also at Kafkas University, Kars, Turkey
- 60: Also at Istanbul Bilgi University, Istanbul, Turkey
- 61: Also at Rutherford Appleton Laboratory, Didcot, United Kingdom
- 62: Also at School of Physics and Astronomy, University of Southampton, Southampton, United Kingdom
- 63: Also at Instituto de Astrofísica de Canarias, La Laguna, Spain
- 64: Also at Utah Valley University, Orem, USA
- 65: Also at Beykent University, Istanbul, Turkey
- 66: Also at Bingol University, Bingol, Turkey
- 67: Also at Erzincan University, Erzincan, Turkey
- 68: Also at Sinop University, Sinop, Turkey
- 69: Also at Mimar Sinan University, Istanbul, Istanbul, Turkey
- 70: Also at Texas A&M University at Qatar, Doha, Qatar
- 71: Also at Kyungpook National University, Daegu, Korea